Cellular/Molecular

Nicotinamide Adenine Dinucleotide-Dependent Binding of the Neuronal Ca^{2+} Sensor Protein GCAP2 to Photoreceptor Synaptic Ribbons

Jagadeesh Kumar Venkatesan,[1]* Sivaraman Natarajan,[1]* Karin Schwarz,[1]* Sabine I. Mayer,[1] Kannan Alpadi,[1] Venkat Giri Magupalli,[1] Ching-Hwa Sung,[2] and Frank Schmitz[1]

[1]Department of Neuroanatomy, Institute for Anatomy and Cell Biology, Saarland University Medical School, 66421 Homburg/Saar, Germany, and [2]Department of Ophthalmology, Cell and Developmental Biology, Margaret M. Dyson Vision Research Institute, Weill Medical College of Cornell University, New York, New York 10021

Guanylate cyclase activating protein 2 (GCAP2) is a recoverin-like Ca^{2+}-sensor protein known to modulate guanylate cyclase activity in photoreceptor outer segments. GCAP2 is also present in photoreceptor ribbon synapses where its function is unknown. Synaptic ribbons are active zone-associated presynaptic structures in the tonically active photoreceptor ribbon synapses and contain RIBEYE as a unique and major protein component. In the present study, we demonstrate by various independent approaches that GCAP2 specifically interacts with RIBEYE in photoreceptor synapses. We show that the flexible hinge 2 linker region of RIBEYE(B) domain that connects the nicotinamide adenine dinucleotide (NADH)-binding subdomain with the substrate-binding subdomain (SBD) binds to the C terminus of GCAP2. We demonstrate that the RIBEYE–GCAP2 interaction is induced by the binding of NADH to RIBEYE. RIBEYE–GCAP2 interaction is modulated by the SBD. GCAP2 is strongly expressed in synaptic terminals of light-adapted photoreceptors where GCAP2 is found close to synaptic ribbons as judged by confocal microscopy and proximity ligation assays. Virus-mediated overexpression of GCAP2 in photoreceptor synaptic terminals leads to a reduction in the number of synaptic ribbons. Therefore, GCAP2 is a prime candidate for mediating Ca^{2+}-dependent dynamic changes of synaptic ribbons in photoreceptor synapses.

Introduction

The guanylate cyclase activating protein 2 (GCAP2) is a recoverin-like neuronal Ca^{2+}-sensor protein highly expressed in photoreceptors (for review, see Koch et al., 2002; Palczewski et al., 2004). Three members of the GCAP family (GCAP1, GCAP2, and GCAP3) are known in the mammalian retina: GCAP1 and GCAP2 are expressed both in rod and cone photoreceptors, whereas GCAP3 is found exclusively in cone photoreceptors (Imanishi et al., 2002). GCAP2 contains four EF-hands from which the first EF-hand is nonfunctional. GCAP2 contains an N-terminal myristoylation signal and is myristoylated *in situ* (Olshevskaya et al., 1997). GCAP2 is well known to modulate the activity of photoreceptor guanylate cyclases in a Ca^{2+}-dependent manner (for review, see Koch et al., 2002). GCAPs are not restricted to outer and inner segments of photoreceptors but are also present in the presynaptic terminals (Otto-Bruc et al., 1997; Duda et al., 2002, Pennesi et al., 2003; Makino et al., 2008). The significance of GCAP2 in the presynaptic terminals is unknown.

Photoreceptor synapses are ribbon-type synapses (for review, see Heidelberger et al., 2005; Sterling and Matthews, 2005; tom Dieck and Brandstätter, 2006). These synapses are tonically active and reliably transmit a broad range of stimulus intensities. Morphologically, ribbon synapses are characterized by the presence of large presynaptic structures, the synaptic ribbons. Synaptic ribbons are anchored in the active zone complex and are associated with numerous synaptic vesicles and also other membranes (for review, see Heidelberger et al., 2005; Sterling and Matthews, 2005; tom Dieck and Brandstätter, 2006). The protein RIBEYE is the major component of synaptic ribbons (Schmitz et al., 2000; Zenisek et al., 2004; Wan et al., 2005; Magupalli et al., 2008). RIBEYE consists of a unique A domain and a B domain that is mostly identical to the protein C-terminal-binding protein 2 (CtBP2) (Schmitz et al., 2000). RIBEYE(B) domain binds nicotinamide adenine dinucleotide (NADH) with high affinity (Schmitz et al., 2000). RIBEYE(B) domain/CtBP2 is highly related to CtBP1 (for review, see Chinnadurai, 2002). The crystal structure of a truncated CtBP1 (tCtBP1) that lacks the hydrophobic C-terminal region (CTR) and a small N-terminal stretch has

Received July 30, 2009; revised March 8, 2010; accepted March 21, 2010.

This work was supported by research grants from the German Research Community Deutsche Forschungsgemeinschaft (SFB530, Teilprojekt C11; GRK1326) and funding from the Saarland University (HOMFOR, ZFK) to F.S., HOMFOR to K.S., and by Research to Prevent Blindness and National Eye Institute-National Institutes of Health Grant EY11307 to C.-H.S. The sequences obtained in the present study for bovine GCAP2 are identical to the sequences of bovine GCAP2 that have been deposited previously at GenBank (L430001.1 and U32856.1). We thank Prof. Jens Rettig, Dr. Ulf Matti, and Carolin Bick (Saarland University, Institute of Physiology) for help with making recombinant Semliki Forest virus.

*J.K.V., S.N., and K.S. contributed equally to this work.

Correspondence should be addressed to Dr. Frank Schmitz at the above address. E-mail: frank.schmitz@uniklinik-saarland.de.

S. I. Mayer's present address: Neuroscience Institute, Stanford School of Medicine, Palo Alto, CA 94304.

K. Alpadi's present address: Department Biochemistry and Molecular Biology, Baylor College of Medicine, Houston, TX 77030.

V. G. Magupalli's present address: Department of Pharmacology, University of Washington, Seattle, WA 98195.

DOI:10.1523/JNEUROSCI.3701-09.2010

 0270-6474/10/306559-18$15.00/0

Table 1. Antibodies and labeling reagents

Antibodies/reagents	Source	Dilution used	Secondary antibody	Dilution used
Antibodies used for Western blotting				
GCAP2 6th immune serum	Rabbit polyclonal	1:1000	GAR-POX; Sigma, cat. #A6154	1:10,000
GCAP2(A1); Santa Cruz Biotechnology, cat. #SC-59543	Mouse monoclonal	1:1000	GAM-POX; Sigma, cat. #A3673	1:10,000
U2656 (Schmitz et al., 2000)	Rabbit polyclonal	1:10,000	GAR-POX; Sigma, cat. #A6154	1:10,000
RIBEYE/CtBP2; BD Transduction Laboratories, cat. #612044	Mouse monoclonal	1:10,000	GAM-POX; Sigma, cat. #A3673	1:10,000
Antibodies used for immunolabeling				
GCAP2 6th immune serum	Rabbit polyclonal	1:500	GAR-Cy3; Zymed, cat. #81-6115	1:1000
GCAP2(A1); Santa Cruz Biotechnology, cat. #SC-59543	Mouse monoclonal	1:1000	GAM-Cy3; Rockland, cat. #610-104-121	1:1000
U2656 (Schmitz et al., 2000)	Rabbit polyclonal	1:1000	GAR-Cy2; Rockland, cat. #611-111-122	1:1000
RIBEYE/CtBP2; BD Transduction Laboratories, cat. #612044	Mouse monoclonal	1:500	GAM-Cy2; Jackson ImmunoResearch, cat. #115-096-146	1:1000
mGluR6; Neuromics/Acris, cat. #RA13105	Rabbit polyclonal	1:500	GAR-Cy3; Sigma, cat. #C 2821	1:1000
SV2 A; Synaptic Systems, cat. #119 00 2	Rabbit polyclonal	1:500	GAR-Cy2; Rockland, cat. #611-111-122	1:1000
Synaptophysin; Sigma, cat. #S5768	Mouse monoclonal	1:500	GAM-Cy2; Jackson ImmunoResearch, cat. #115-096-146	1:1000
Antibodies used for whole-mount immunostaining				
U2656 (Schmitz et al., 2000)	Rabbit polyclonal	1:500	GAR-Cy3; Zymed, cat. #81-6115	1:1000
Reagent used for PNA labeling				
Lectin PNA from *Arachis hypogaea*[a]	Lectin PNA; Invitrogen cat. #L-21409	1:250		

Antibodies used for *in situ* proximity ligation assays are summarized in detail in Materials and Methods. cat., Catalog; GAR, goat anti-rabbit; GAM, goat anti-mouse; PNA, peanut agglutinin.

[a]Alexa Fluor 488 conjugate.

been resolved (Kumar et al., 2002; Nardini et al., 2003). CtBP proteins (including RIBEYE) belong to a family of D-isomer-specific 2-hydroxyacid dehydrogenases (for review, see Chinnadurai, 2002). Structural analyses of this class of proteins demonstrated the presence of two distinct subdomains: a central NADH-binding subdomain (NBD) and the bipartite substrate-binding subdomain (SBD) (Kumar et al., 2002; Nardini et al., 2003). SBD and NBD are connected by two flexible hinge regions, hinge 1 and hinge 2. Hinge 1 connects the N-terminal portion of the SBD (SBDa) with the NBD; hinge 2 connects the NBD with the C-terminal portion of the SBD (SBDb) (for review, see Chinnadurai, 2002). After NADH binding, NBD and SBD move relative to each other and adopt a "closed" conformation (Lamzin et al., 1994; Nardini et al., 2003).

Ca^{2+}- and illumination-dependent synaptic ribbon dynamics have been described previously (Spiwoks-Becker et al., 2004). However, the underlying mechanism is unclear. We identified GCAP2 as a RIBEYE-interacting protein that could mediate Ca^{2+}-dependent synaptic ribbon dynamics.

Materials and Methods

Materials

Plasmids

Details on all plasmids used in the present study are posted in the supplemental material (available at www.jneurosci.org).

Bacterial strains

The *Escherichia coli* DH10B genotype is F-*mcr*A Δ(*mrr-hsd*RMS-*mcr*BC) Φ80*lacZ*ΔM15 Δ*lac*X74 *rec*A1 *end*A1 *ara*D139 Δ(*ara, leu*)7697 *gal*U *gal*Kλ-*rps*L *nup*G. The *E. coli* BL21(DE 3) genotype is [F^- *omp*T *hsd*S_B ($r_B^- m_B^-$) *gal dcm* (DE3)].

Antibodies

A polyclonal antibody against full-length bovine GCAP2-fusion protein was generated in rabbits by using purified, bacterially expressed glutathione-*S*-transferase (GST)-tagged full-length bovine GCAP2(amino acids 1-204) as antigen. The sixth immune bleed (obtained 90 d after initial immunization) was used in the present experiments. A mouse monoclonal antibody against human GCAP2 that reacts with bovine GCAP2 but not with bovine GCAP1 (supplemental Fig. 3*F*, available at www.jneurosci.org as supplemental material) was purchased from Santa Cruz Biotechnology (clone A1, sc-59543). Two antibodies against RIBEYE were used in the present study: one rabbit polyclonal antibody (U2656) (Schmitz et al., 2000) and one monoclonal antibody against RIBEYE(B) domain/CtBP2 (BD Transduction Laboratories) (Alpadi et al., 2008). Additional antibodies used in the present study are mouse monoclonal anti-GST (Sigma) and mouse monoclonal anti-maltose-binding protein (anti-MBP; New England Biolabs). More details on the antibodies used are given in Table 1.

Methods

Yeast-two-hybrid methods

Yeast-two-hybrid (YTH) methods (generation of electrocompetent yeasts, electroporation of yeasts, and yeast matings) were performed exactly as described previously (Alpadi et al., 2008; Magupalli et al., 2008).

Fusion protein expression and purification

Fusion protein was expressed in BL21(DE3) as described previously (Schmitz et al., 2000; Magupalli et al., 2008; Alpadi et al., 2008).

Fusion protein pull-down experiments

Fusion protein pull-down experiments were performed as described previously (Alpadi et al., 2008; Magupalli et al., 2008). For fusion protein pull-down experiments, purified GST-tagged proteins (GST-GCAP2 and GST) were used as immobilized bait proteins, and eluted MBP-tagged proteins [RIBEYE(B)-MBP and MBP alone] as soluble prey proteins. GST and MBP alone served as control proteins. In the pull-down assays, all fusion proteins were used at an equimolar concentration of ~0.8 μM in a volume of 500 μl incubation buffer containing 100 mM Tris, pH 8.0, 150 mM NaCl, 1 mM EDTA, 0.25% (w/v) Triton X-100 (Tx-100), and 1 mM β-mercaptoethanol (βME) if not denoted otherwise. After a 5–6 h incubation at 4°C, samples were washed by repeated centrifugation of the beads (3000 rpm, 2 min, 4°C) and subsequent resuspension with PBS. This procedure was repeated three times. Afterward, the final pellets were boiled with SDS-sample buffer (96°C, 5 min) and subjected to SDS-PAGE.

Preabsorption experiments

Preabsorption for Western blotting. Fifty microliters of GCAP2 immune serum (sixth immune serum) were added to GST-GCAP2 (20 μg) and GST (20 μg) fusion protein bound to beads in a final volume of ~75 μl and incubated overnight at 4°C in an overhead rotator. After incubation, samples were centrifuged at 13,000 rpm for 3 min at 4°C and the respective supernatants were taken for the subsequent experiments. For Western blot analyses of the bovine retina extract, the two preabsorbed antisera described above were used at a dilution of 1:1000 in blocking buffer (5% skim milk powder in PBS).

Preabsorption for immunofluorescence. Preabsorption with fusion protein for immunofluorescence microscopy was done as described above for Western blotting. The preabsorbed antisera (preabsorbed either with

GST or GCAP2-GST) were subsequently tested at identical dilutions for immunolabeling on cryostat sections of the bovine retina.

Coimmunoprecipitation analyses using extracts from the bovine retina

Experiments were performed mostly as described previously (Alpadi et al., 2008). In brief, for each assay, one freshly isolated bovine retina was incubated in 1 ml lysis buffer, containing 100 mM Tris-HCl, pH 8.0, 150 mM NaCl, 1 mM EDTA, and 1% Tx-100 for 45 min on ice. The sample was mechanically cracked by forcefully ejecting the retinal lysate through a 20 gauge needle. This procedure was repeated 10 times. After lysis, the extract was centrifuged at 13,000 rpm (Biofuge Fresco; Heraeus; #3329 rotor) for 30 min at 4°C. This centrifugation step was repeated once. Afterward, the lysate (see Fig. 4, "bovine retina lysate") was precleared by the addition of 15 μl of preimmune serum and 20 μl of washed protein A-Sepharose beads (2 h incubation at 4°C with an overhead rotator). Next, samples were centrifuged at 13,000 rpm for 30 min at 4°C. The supernatant was split in two equal volumes, for the control and experimental assays. For the control assay, 15 μl of GCAP2 or RIBEYE preimmune serum was added; for the experimental assay, 15 μl of GCAP2 or RIBEYE immune serum was added and incubated overnight at 4°C using an overhead rotator. After overnight incubation, the assays were washed thrice by repeated centrifugation (3000 rpm, 1 min, 4°C) and resuspension with 1 ml of incubation buffer. The final pellet was boiled in 20 μl sample buffer, subjected to SDS-PAGE, and analyzed by Western blotting with the indicated antibodies.

Purification of synaptic ribbons

Purification of synaptic ribbons was performed as described previously (Schmitz et al., 1996, 2000; Alpadi et al., 2008; Magupalli et al., 2008). Purified ribbons were checked for their enrichment with RIBEYE, absence for synaptophysin, and presence of a high density of horseshoe-shaped synaptic ribbons by immunofluorescence microscopy of the synaptic ribbon fractions with antibodies against RIBEYE (U2656) (supplemental Fig. 3*D*,*E*, available at www.jneurosci.org as supplemental material). Bovine eyes were obtained from a local slaughterhouse.

Immunolabeling analyses

Immunolabeling analyses of retinal sections and fractions were performed as described previously (Schmitz et al., 2000, 2006; Alpadi et al., 2008) using a Zeiss inverted Axiovert 200 M microscope equipped for conventional epifluorescence microscopy. In brief, 10-μm-thick cryostat sections were heat fixed for 10 min at 50°C and subsequently treated with 0.5% BSA for 1 h at room temperature (RT) before the primary antibodies were applied at the indicated dilutions (see also Table 1). Primary antibodies were usually applied overnight at 4°C if not indicated otherwise. After removing unbound antibody by several washes with PBS, secondary antibodies were applied at the dilutions in PBS given in Table 1 (1 h, RT). After removing unbound antibody with PBS sections were mounted in *N*-propyl gallate (NPG) antifade (Magupalli et al., 2008). Incubations only with secondary antibody (without primary antibody) served as negative controls. Additional details of the applied antibodies are given in Table 1. Sections were analyzed with a Zeiss Axiovert 200 M microscope equipped with an apotome and the respective filter sets (Ex BP 450–490 nm/BS FT510/EM BP 515-565; EX BP 546/12/BS FT 580/EM LP 590). Confocal sections were obtained with an LSM710 confocal laser scanning microscope (Zeiss). Images were captured using a 63× objective (1.4 numerical aperture) with the ZEN2009 software.

Double-labeling of cryostat sections of the bovine retina with GCAP2 antibodies and Peanut agglutinin

Cryosections of bovine retina were heat fixed for 10 min at 50°C and incubated with blocking buffer (containing 0.5% BSA, 0.02% Tx-100 in PBS) at RT for 45 min. Sections were then incubated with primary polyclonal GCAP2 antibody at a 1:500 dilution in blocking buffer overnight at 4°C. After brief washing with blocking buffer, sections were incubated with secondary antibody GAR-CY3 (1 h, RT). Section were next incubated with Peanut agglutinin–Alexa 488 (1:250 dilution) in blocking buffer for 3 h at RT. After washing once with PBS, sections were mounted in NPG-antifade for microscopic analysis.

Generation of recombinant Semliki Forest virus

Cell culture. Baby hamster kidney-21 (BHK-21) cells were cultured in OPTIMEM/GlutaMax medium (Invitrogen) supplemented with 10% (v/v) tryptose phosphate broth, 20 mM HEPES, 2.5% FCS at 37°C, 5% CO_2, and used between passage numbers 5 to 25.

Generation of recombinant SFV particles. The Semliki forest (SLF) virus expression vector GCAP2-EGFPpSFV was constructed in three steps. First, PCR was used to generate a *Bgl*II-*Bam*HI-flanked enhanced green fluorescent protein (EGFP) fragment using the following forward and reverse primers: 5′-TTTAGATCTGCCACCATGGTGAGCAAGGGCGA (forward) and 5′-TTTGGATCCCTTGTACAGCTCGTCCAT (reverse) for ligation into the *Bam*HI site of the pSFV1 expression vector. Next, a B*am*HI-*Bss*HII-flanking GCAP2 insert was amplified by PCR (5′-TTTTG-GATCCATGGGGCAGCAGTTCAGC, forward primer; 5′- TTTTGC-GCGCTCAGAACATGGCACTTTTCC, reverse primer) using GCAP2(amino acids 1-204)pGEX as a template. The PCR product was cloned into the *Bam*HI-*Bss*HII site of EGFPpSFV (Ashery et al., 1999). The internal ribosomal entry site of pSFV was deleted by digestion with *Bss*HII-*Cla*I, fill in with Klenow, and religation of the vector. EGFPpSFV was used as control plasmid/control virus (Ashery et al., 1999). mRNA was generated from the pSFV1 expression vector (GCAP2-EGFPpSFV; EGFPpSFV) and pSFV2 helper vector by linearizing both vectors with *Spe*I and *in vitro* transcription using SP6 RNA polymerase according to the manufacturer's instructions (mMessage mMachine SP6 Kit; Ambion). Ten micrograms of purified mRNA were electroporated into 1×10^7 BHK-21 cells in OPTIMEM/GlutaMax medium without supplements at 360 V, 75 μF and pulsed twice using a Bio-Rad GenePulser II apparatus. Cells were resuspended in 10 ml of complete OPTIMEM/GlutaMax growth medium (see above, Cell culture) and plated for 24 h at 31°C, 5% CO_2. Medium was recovered from the flasks and centrifuged at 400 × *g* for 5 min. The supernatants were aliquoted and stored at −80°C. Virus titer was determined exactly as described previously (Ashery et al., 1999).

Infection of mouse organotypic retinal cultures. The virus-containing stock was supplemented with an equal volume of OPTIMEM/GlutaMax containing 0.2% BSA. Virus was activated by the addition of chymotrypsin (0.2 mg/ml; Sigma-Aldrich) and subsequent incubation for 40 min at room temperature. Proteolytic activation of the virus was stopped by the addition of aprotinin (0.6 mg/ml; Sigma-Aldrich). Organotypic retina cultures were incubated with the respective virus ($4–5 \times 10^7$ infectious units/ml). After 16–24 h at 31°C, 5% CO_2, the virus-containing medium was replaced by normal growth medium.

Organotypic culture of retinal explants

Preparation of organotypic cultures was performed mostly as described previously (Fischer et al., 2000; Pérez-León et al., 2003; Zhang et al., 2008), with some modifications. Briefly, freshly isolated eyes enucleated from adult mice housed under ambient light conditions were immediately immersed into ice-cold RPMI 1640 (supplemented with 10% fetal calf serum, 10 mM HEPES, 2 mM L-glutamine, 1 mM sodium pyruvate, 50 μM βME, 100 U/ml penicillin, and100 μg/ml streptomycin). The anterior portion of the eye was removed by incision along the ora serrata. After removal of lens and vitreous body, the optic nerve was cut and the retina subsequently gently removed from the posterior eyecup. The retina was mounted photoreceptor side down on polyethylene terephthalate cell culture inserts (8.0 μm pore size; Falcon) placed in six-well plates containing 1 ml of RPMI 1640 with the above described supplements. Explants were incubated for 1 h at 31°C, 5%CO_2, and then infected with recombinant Semliki Forest virus. For infection with recombinant Semliki Forest virus, RPMI 1640 medium was replaced by 1 ml of the activated virus solution (see above; virus titer typically between $4–5 \times 10^7$ infectious units per ml) and incubated overnight at 31°C, 5% CO_2. After 16–24 h of infection, the virus-containing medium was removed from the cell culture dishes by three washes with RPMI (with supplements). The explants were allowed to recover for several hours before being processed for whole-mount immunostaining.

Whole-mount immunostaining of organotypic retinal explants

One day after infection, retinal explants were fixed in 4% paraformaldehyde (PFA) for 20 min at 4°C. Explants were permeabilized for 30 min at

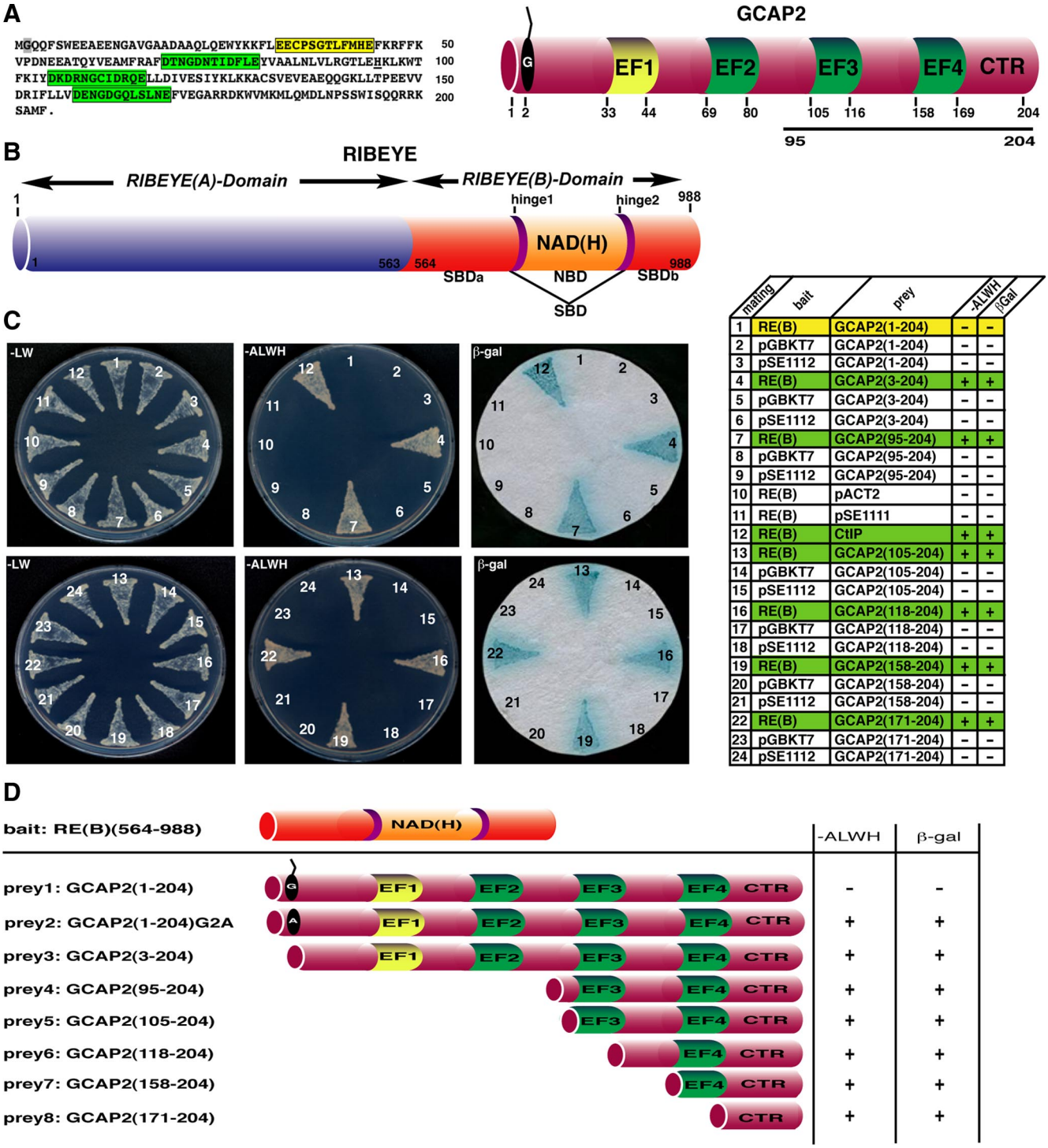

mating	bait	prey	-ALWH	βGal
1	RE(B)	GCAP2(1-204)	–	–
2	pGBKT7	GCAP2(1-204)	–	–
3	pSE1112	GCAP2(1-204)	–	–
4	RE(B)	GCAP2(3-204)	+	+
5	pGBKT7	GCAP2(3-204)	–	–
6	pSE1112	GCAP2(3-204)	–	–
7	RE(B)	GCAP2(95-204)	+	+
8	pGBKT7	GCAP2(95-204)	–	–
9	pSE1112	GCAP2(95-204)	–	–
10	RE(B)	pACT2	–	–
11	RE(B)	pSE1111	–	–
12	RE(B)	CtIP	+	+
13	RE(B)	GCAP2(105-204)	+	+
14	pGBKT7	GCAP2(105-204)	–	–
15	pSE1112	GCAP2(105-204)	–	–
16	RE(B)	GCAP2(118-204)	+	+
17	pGBKT7	GCAP2(118-204)	–	–
18	pSE1112	GCAP2(118-204)	–	–
19	RE(B)	GCAP2(158-204)	+	+
20	pGBKT7	GCAP2(158-204)	–	–
21	pSE1112	GCAP2(158-204)	–	–
22	RE(B)	GCAP2(171-204)	+	+
23	pGBKT7	GCAP2(171-204)	–	–
24	pSE1112	GCAP2(171-204)	–	–

Figure 1. RIBEYE interacts with GCAP2 in the YTH system. ***A***, Sequence of bovine GCAP2 given in the single letter amino acid code. The four EF- hands of GCAP2 are indicated in color. EF-hand 1 (yellow) is nonfunctional and does not bind Ca^{2+}; EF-hands 2–4 (green) are functional and bind Ca^{2+}. The bold bar that underlines the schematic drawing of GCAP2 denotes the extension of the initially obtained GCAP2 prey clone (also in ***D***, prey 4). Glycine G2 (gray) is myristoylated *in situ*. ***B***, Schematic domain depiction of RIBEYE. RIBEYE consists of an N-terminal A domain and a C-terminal B domain. The B domain can be further subdivided into a contiguous central NBD and a discontinuous SBD. The SBD consists of two sequence stretches, SBDa and SBDb, that are linked to the NBD via two flexible hinge regions, hinge 1 and hinge 2 (see also Figs. 2*A*, *B*, 8*D*, *E*; supplemental Fig. 2*A*, available at www.jneurosci.org as supplemental material). The structure model of RIBEYE(B) (see Fig. 2*A*, *B*) (Alpadi et al., 2008; Magupalli et al., 2008) covers the region from amino acids 575 to 905 of RIBEYE. The hydrophobic C-terminal region of RIBEYE(B) ranging from amino acids 912 to 988 is denoted as the CTR of RIBEYE in the text. ***C***, GCAP2 interacts with RIBEYE(B) [RE(B)] in the YTH system. Summary plates of YTH analyses obtained with the indicated bait and prey plasmids are shown. For convenience, experimental bait–prey pairs are shown in color (green, interacting bait–prey pairs; yellow, noninteracting bait–prey pairs); control matings are not colored. RIBEYE(B) interacts with GCAP2 as judged by growth on selective plates (−ALWH) and expression of β-galactosidase (β-gal) activity (yeast matings 4, 7, 13, 16, 19, and 22). The respective control matings (autoactivation controls; yeast matings 2, 3, 5, 6, 8–11, 14, 15, 17, 18, 20, 21, 23, 24) did not show growth on the −ALWH plate and no expression of β-galactosidase activity. Growth on −LW plates demonstrates the presence of the bait and prey plasmids in the mated yeasts. Full-length GCAP2 containing an intact myristoylation site did not interact with RIBEYE(B) (mating 1) because the myristoylation prevents the entry of the prey protein into the nucleus (see text). If the myristoylation signal is deleted by a point mutation (G2A), full-length GCAP2 also interacts with RIBEYE(B) (supplemental Fig. 1*A*, available at www.jneurosci.org as supplemental material). Similarly, deleting the myristoylation signal by truncation of the first two amino acids (*Figure legend continues*.)

RT in incubation buffer (PBS with 0.3% Tx-100 and 0.5% BSA) and subsequently incubated with primary antibody (U2656, 1:500 dilution in incubation buffer) overnight at 4°C. Unbound antibody was removed by intensive washing with washing buffer (PBS, 0.5% Tween-20, 0.5% BSA). Explants were then incubated with the indicated fluorophore-conjugated secondary antibody (1:1000 in incubation buffer) (Table 1) overnight at 4°C. Unbound antibody was again removed by intensive washing with washing buffer. Explants were then fixed with 4% PFA (15 min, 4°C), cut with a cryostat (10-μm-thick sections), and thawed on uncoated Superfrost coverslides. Sections were analyzed with a Zeiss Axiovert 200 M microscope equipped with an apotome and the respective filter sets (EX BP 450–490 nm/BS FT510/EM BP 515-565; EX BP 546/12/BS FT 580/EM LP 590). For counting, terminals were observed in the apotome mode.

Three-dimensional reconstruction of immunolabeled structures in retinal explants

For three-dimensional (3D) reconstructions, retina sections were observed with the Zeiss Axiovert 200 M microscope. Z-stacks were taken using the apotome and 3D-reconstruction was performed using the Inside4D software module from Zeiss.

Electron microscopy

Electron microscopy of organotypical retinas was performed as described previously (Schmitz et al., 1996, 2000; Schoch et al., 2006).

In situ *proximity ligation assays*

Proximity ligation assays (PLAs) are a highly sensitive and specific way to detect protein–protein interaction *in situ*, e.g., in tissue sections (Gustafsdottir et al., 2005; Söderberg et al., 2006, 2008). Proximity ligation reactions critically depend on the distance of the two interaction partners. Positive PLA interaction signals indicate that the interacting proteins are localized in <40 nm distance from each other (Söderberg et al., 2006). PLA components (Gustafsdottir et al., 2005) were purchased from Eurogentec and performed according to the manufacturer's instructions. The following components were purchased from Eurogentec: anti-rabbit immunoglobulins coupled to the "PLUS" oligonucleotide (PLA PLUS probe), anti-mouse immunoglobulins coupled to the PLA "MINUS" probe, and the fluorescence detection kit 563 containing the linker oligonucleotide, enzymes for rolling circle amplification, and fluorescent probe for product detection.

In brief, 10-μm-thick sections of flash-frozen mouse eyes (prepared as described above) were heat fixed for 10 min at 50°C and subsequently treated with the Duolink blocking solution supplied by the manufacturer (Olink Biosciences) for 30 min at 37°C. Next, sections were incubated with primary antibody dilutions (in Duolink antibody dilution solution; Olink Bioscience, Eurogentec). The following antibodies were used at the indicated dilutions: polyclonal rabbit GCAP2 antibody (1:500); monoclonal anti-RIBEYE(B)/CtBP2 (BD Biosciences; 1:500); polyclonal rabbit RIBEYE antibody (U2656, 1:500); mouse monoclonal antibody against opsin (Rho1D4, 1:500); polyclonal antibody against mGluR6 (Neuromics/Acris Antibodies; RA13105; 1:500). Duolink *in situ* PLAs were performed as described by the manufacturer: After incubation with the primary antibodies, combinations of the PLA probes (anti-rabbit PLUS probe, anti-mouse MINUS probe, both diluted 1:8 in Duolink antibody dilution buffer) were added to the sections for 2 h at 37°C in a wet chamber. After washing the sections with TBS (two times for 5 min each), hybridization with the linker oligonucleotide was performed for 15 min at 37°C. Tissue was washed for 1 min with TBS before ligation was performed for 15 min at 37°C in a humid chamber. After washes with TBS for 5 min, rolling circle amplification was done for 90 min at 37°C precisely following the manufacturer's protocol. The product of the rolling circle amplification was detected with the Duolink detection kit 563 (Olink Bioscience, purchased via Eurogentec) using Duolink fluorophore 563-labeled oligonucleotide diluted 1:5 with H_2O. The detection reaction was performed for 60 min at 37°C. As negative controls, PLAs were done without primary antibodies or with only one primary antibody. Sections were subsequently washed with 2× SSC (2 min), 1× SSC (2 min), 0.2× SSC (2 min), and 0.02× SSC (1 min). Afterward, sections were mounted with Duolink mounting medium, sealed with a coverslip and analyzed by epifluorescence microscopy as described above. As an additional control to test for the spatial sensitivity/proximity requirements of the *in situ* PLA reactions, we also analyzed for PLA signals between a presynaptic marker (RIBEYE) and a postsynaptic marker at the tips of invaginating ON bipolar cells (mGluR6) (see Fig. 7*M*). As positive controls, we used a combination of the following two antibodies [rabbit polyclonal RIBEYE U2656/mouse anti-RIBEYE(B)/CtBP2] (see Fig. 7*L*) and mouse monoclonal anti-opsin (Rho1D4/rabbit polyclonal GCAP2) (see Fig. 7*K*). The antibodies that were used in the Olink PLAs are summarized as follows with their indicated working dilutions: rabbit polyclonal GCAP2 antibody (1:500); rabbit polyclonal antibody against RIBEYE U2656 (1:500); rabbit polyclonal antibody against mGluR6 (1:500); mouse monoclonal antibody against RIBEYE(B)/CtBP2; mouse monoclonal antibody against opsin (Rho1D4) (1:500). Antibody combinations were used as indicated in Figure 7.

Results

The C terminus of GCAP2 interacts with the hinge 2 region of RIBEYE(B)

In a YTH screen using RIBEYE(B) as bait construct, we identified GCAP2 as a potential interaction partner of RIBEYE (Fig. 1; supplemental Fig. 1, available at www.jneurosci.org as supplemental material). The GCAP2 prey clone we obtained started at histidine H95 of bovine GCAP2 [GCAP2(95-204)] and coded for the two C-terminal EF-hands and the CTR of GCAP2 (Fig. 1*D*, prey 4). The prey clone was not autoactivating as judged by the respective control matings (Fig. 1*C*), thus pointing to an interaction between RIBEYE and GCAP2 in the YTH system. To further consolidate these findings, we cloned full-length GCAP2 and the indicated GCAP2 constructs from bovine retinal cDNA (Fig. 1*C*,*D*) into the respective yeast vectors and tested them for interaction with RIBEYE(B) in the YTH system. The GCAP2 constructs (Fig. 1*D*) were designed based on the known domain structure of GCAP2 (Ames et al., 1999). All of the tested GCAP2 constructs (except for full-length GCAP2 with an intact N-terminal myristoylation signal) interacted with RIBEYE(B) (Fig. 1*C*,*D*; supplemental Fig. 1*A*, available at www.jneurosci.org as supplemental material). If the N-terminal myristoylation signal in full-length GCAP2 (encoded by the first N-terminal amino acids, methionine and glycine) was deleted either by point-mutating glycine 2(G2) into alanine (G2A) or by deleting the first two N-terminal amino acids, GCAP2 interacted with RIBEYE(B) in the YTH system (Fig. 1*C*,*D*; supplemental Fig. 1*A*,*B*, available at www.jneurosci.org as supplemental material). Thus, the myristoylation of GCAP2 at glycine G2 and the resulting membrane association prevent GCAP2 from entering the nucleus where the interaction needs to take place in the Gal4-based YTH system. The mapping analyses revealed that RIBEYE interacted with GCAP2 even when all EF-hands of GCAP2 were deleted by N-terminal truncations (Fig. 1*C*,*D*). The C-terminal region of GCAP2 that starts after the fourth EF-hand (abbreviated as CTR in the following text) retained the capability to interact with RIBEYE(B) in the YTH system. Therefore, we conclude that the CTR of GCAP2 mediates the interaction with RIBEYE. This assumption is further supported by our finding that point mutants of the CTR of GCAP2 no longer interacted with RIBEYE(B) (sup-

←

(*Figure legend continued.*) also results in interaction between RIBEYE(B) and GCAP2 (mating 4). Mating 12 is an unrelated positive control mating (Alpadi et al., 2008). ***D***, Schematic summary of the mapping analyses obtained with the YTH system. RIBEYE(B) interacts with all tested GCAP2 constructs except for full-length GCAP2 that contains an intact myristoylation signal (prey 1). If the myristoylation signal is deleted by a point mutation (G2A) (prey 2), full-length GCAP2 also interacts with RIBEYE(B) (supplemental Fig. 1*A*, available at www.jneurosci.org as supplemental material). ALWH, Dropout medium lacking adenine, leucine, tryptophan, and histidine; LW, dropout medium lacking leucine and tryptophan.

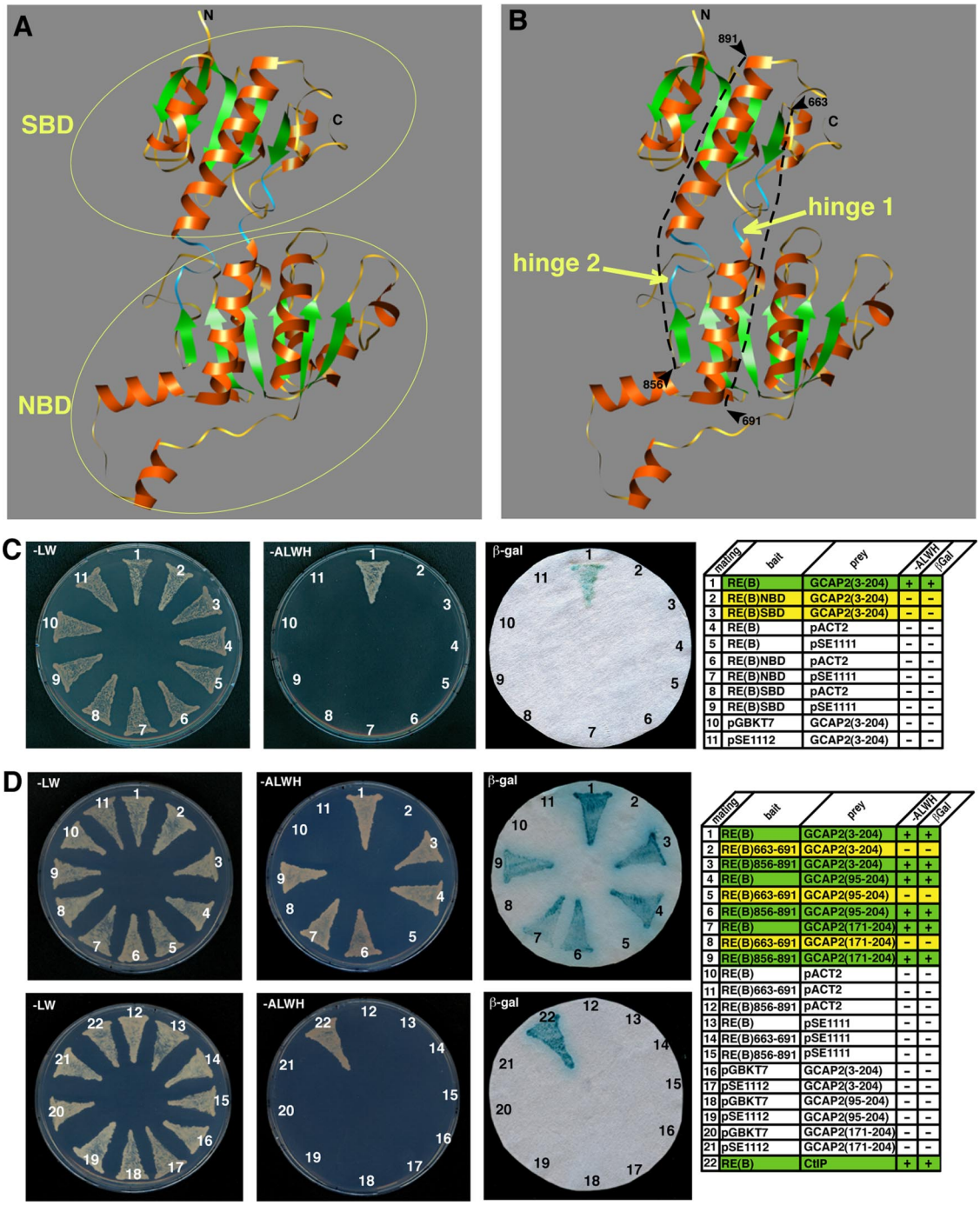

mating	bait	prey	-ALWH	/Gal
1	RE(B)	GCAP2(3-204)	+	+
2	RE(B)NBD	GCAP2(3-204)	–	–
3	RE(B)SBD	GCAP2(3-204)	–	–
4	RE(B)	pACT2	–	–
5	RE(B)	pSE1111	–	–
6	RE(B)NBD	pACT2	–	–
7	RE(B)NBD	pSE1111	–	–
8	RE(B)SBD	pACT2	–	–
9	RE(B)SBD	pSE1111	–	–
10	pGBKT7	GCAP2(3-204)	–	–
11	pSE1112	GCAP2(3-204)	–	–

mating	bait	prey	-ALWH	/Gal
1	RE(B)	GCAP2(3-204)	+	+
2	RE(B)663-691	GCAP2(3-204)	–	–
3	RE(B)856-891	GCAP2(3-204)	+	+
4	RE(B)	GCAP2(95-204)	+	+
5	RE(B)663-691	GCAP2(95-204)	–	–
6	RE(B)856-891	GCAP2(95-204)	+	+
7	RE(B)	GCAP2(171-204)	+	+
8	RE(B)663-691	GCAP2(171-204)	–	–
9	RE(B)856-891	GCAP2(171-204)	+	+
10	RE(B)	pACT2	–	–
11	RE(B)663-691	pACT2	–	–
12	RE(B)856-891	pACT2	–	–
13	RE(B)	pSE1111	–	–
14	RE(B)663-691	pSE1111	–	–
15	RE(B)856-891	pSE1111	–	–
16	pGBKT7	GCAP2(3-204)	–	–
17	pSE1112	GCAP2(3-204)	–	–
18	pGBKT7	GCAP2(95-204)	–	–
19	pSE1112	GCAP2(95-204)	–	–
20	pGBKT7	GCAP2(171-204)	–	–
21	pSE1112	GCAP2(171-204)	–	–
22	RE(B)	CtIP	+	+

Figure 2. GCAP2 interacts with the flexible hinge 2 region of RIBEYE(B) [RE(B)] but not with the NBD and SBD alone. ***A***, ***B***, Structure model of the B domain of RIBEYE based on the crystal structure of tCtBP1 (Kumar et al., 2002; Nardini et al., 2003; see also Alpadi et al., 2008; Magupalli et al., 2008). The structure model covers large parts of the B domain [RE(B)575-905]. The B domain of RIBEYE consists of an NBD and an SBD, which are connected by two flexible hinge regions, hinge 1 and hinge 2 (blue). The dotted lines indicate the extensions of the hinge 1 and hinge 2 constructs tested in ***D*** with the YTH system. ***C***, GCAP2 does not interact with the NBD of RIBEYE(B) or the SBD of RIBEYE(B). Summary plates of YTH analyses obtained with the indicated bait and prey plasmids. For convenience, experimental bait–prey pairs are underlayered in color (green, interacting bait–prey pairs; yellow, noninteracting bait–prey pairs); control matings are not colored. GCAP2 interacts with intact RIBEYE(B) as judged by growth on selective plates (−ALWH) and expression of β-galactosidase (β-gal) activity (yeast mating 1; positive control). In contrast, GCAP2 does not interact either with the NBD (mating 2) or the SBD (mating 3) of RIBEYE alone. The respective control matings (autoactivation controls; yeast matings 4-11) did not show growth on −ALWH plates and no expression of β-galactosidase activity. Growth on −LW plates demonstrates the presence of the bait and prey plasmids in the mated yeasts. ***D***, GCAP2 interacts with the hinge 2 region of RIBEYE(B). Summary plates of YTH analyses obtained with the indicated bait and prey plasmids. For convenience, experimental bait–prey pairs are underlayered in color (green, interacting bait–prey pairs; yellow, noninteracting bait–prey pairs); control matings are not colored. GCAP2 interacts with the hinge 2 region of RIBEYE(B) [RE(B)856-891, yeast matings 3, 6, 9] but not with the hinge1 region of RIBEYE(B) [RE(B)663-691, yeast matings 2, 5, 8] as judged by growth on selective plates (−ALWH) and expression of β-galactosidase activity. The respective control matings (autoactivation controls; yeast matings #10-21) did not show growth on -ALWH plate and expression of β-galactosidase activity. Growth on −LW plates demonstrates the presence of the bait and prey plasmids in the mated yeasts. Matings 1, 4, and 7 represent positive control matings [RE(B)–GCAP2; see also Fig. 1]. Mating 22 represents an unrelated positive control mating (Alpadi et al., 2008). N, N terminus; C, C terminus. ALWH, Dropout medium lacking adenine, leucine, tryptophan, and histidine; LW, dropout medium lacking leucine and tryptophan.

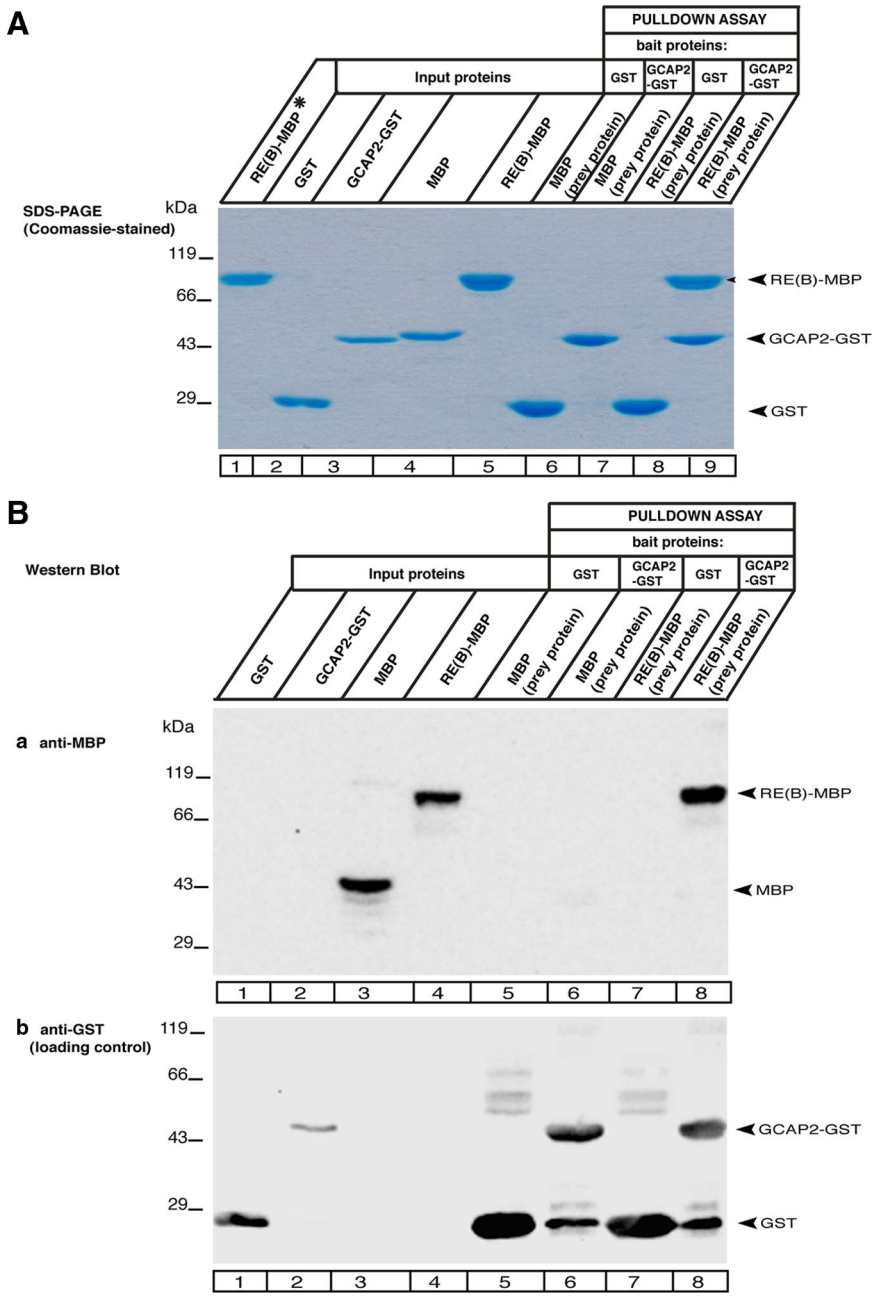

Figure 3. GCAP2 interacts with RIBEYE(B) [RE(B)] in protein pull-down analyses. GCAP2-GST and GST alone (control protein) were used as immobilized bait proteins, and RIBEYE(B)-MBP and MBP alone (control protein) as soluble prey proteins. After incubation and subsequent washing of the immobilized proteins, binding of the soluble prey proteins to the immobilized bait proteins was tested by SDS-PAGE (10% polyacrylamide gels; ***A***) or Western blotting with the indicated antibodies (***B***). ***A***, RIBEYE(B)-MBP binds to GCAP2-GST (lane 9, arrowhead) but not to GST alone (lane 8). MBP alone does not bind to either GCAP2-GST (lane 7) or GST alone (lane 6). Fifteen percent of the total proteins were loaded in the input lanes (lanes 2–5); 100% of the immobilized protein pellets were loaded (lanes 6–9). Eight percent of the unbound fraction (marked by asterisk) was loaded in lane 1. ***Ba***, RIBEYE(B)-MBP binds to GCAP2-GST (lane 8, arrowhead) but not to GST alone (lane 7). ***Bb***, The same blot as in Figure ***Ba*** but after stripping and reprobing of the nitrocellulose with anti-GST antibodies to show equal loading of bait proteins. In ***Ba*** and ***Bb***, 10% of the input (lanes 1–4) was loaded. Always 100% of the immobilized protein pellets were loaded (lanes 5–8).

plemental Fig. 1*B*, available at www.jneurosci.org as supplemental material).

To map the parts of RIBEYE(B) that are important for the interaction with GCAP2, we tested whether the SBD and NBD of RIBEYE(B) alone can interact with GCAP2. Surprisingly, both the SBD and NBD alone did not interact with GCAP2 in the YTH system (Fig. 2*A*,*C*). Since the applied NBD and SBD constructs did not contain the connecting hinge regions, hinge 1 and hinge 2, we tested next whether the hinge regions of RIBEYE(B) might mediate interaction with GCAP2. Indeed, the hinge 2 region (amino acids 856-891) of RIBEYE(B) interacted with GCAP2, whereas the hinge 1 region (amino acids 663-691) did not (Fig. 2*B*,*D*). Therefore, the flexible hinge 2 region that connects the NBD with the SBDb is the essential binding site for GCAP2 (Fig. 2*B*,*D*). This assumption is further supported by the analysis of point mutants of the hinge 2 region, i.e., RIBEYE(B)W867E and RIBEYE(B)T865S (supplemental Fig. 2*A*,*B*, available at www.jneurosci.org as supplemental material). These points mutants of the hinge 2 region of RIBEYE(B) no longer interacted with GCAP2 in the YTH system (supplemental Fig. 2*A*,*B*, available at www.jneurosci.org as supplemental material). In contrast, various point mutants on the outer face of the NBD of RIBEYE(B) (Alpadi et al., 2008; Magupalli et al., 2008) did not affect the binding of GCAP2 (supplemental Fig. 2*C*, available at www.jneurosci.org as supplemental material).

The interaction between RIBEYE and GCAP2 was also observed when full-length RIBEYE(AB) [instead of RIBEYE(B) alone] was used as bait in the YTH analyses (supplemental Fig. 1*C*, available at www.jneurosci.org as supplemental material) indicating that the A domain of RIBEYE does not prevent the interaction between RIBEYE(B) and GCAP2. RIBEYE(B) is known to homodimerize (Magupalli et al., 2008). Analyses of a RIBEYE(B)-dimerization deficient mutant, [RIBEYE(B)ΔHDL] (Magupalli et al., 2008) revealed that RIBEYE(B)–GCAP2 interaction does not require RIBEYE(B) homodimerization. RIBEYE(B)ΔHDL interacted with GCAP2 in the YTH system (supplemental Fig. 1*D*, available at www.jneurosci.org as supplemental material), demonstrating that GCAP2 can interact with monomeric RIBEYE(B).

Confirmation of RIBEYE–GCAP2 interaction by various independent assays

The YTH analyses demonstrated RIBEYE–GCAP2 interaction in the YTH system. To verify this interaction by additional independent approaches, we first performed fusion protein pull-down analyses (Fig. 3). GST-tagged GCAP2 was used as an immobilized bait protein. GST alone served as control protein. RIBEYE(B)-MBP or MBP alone (control protein) was used as the soluble prey protein. GST-GCAP2 (but not GST alone) pulled down RIBEYE(B)-MBP (but not MBP alone), demonstrating a specific direct physical interaction between RIBEYE(B) and GCAP2 (Fig.

3). Based on semiquantitative evaluation, GCAP2-GST pulled down at least ~15% of total RIBEYE(B)-MBP in these experiments (supplemental Fig. 7*C*, available at www.jneurosci.org as supplemental material). Using quantification of the bound proteins (supplemental Fig. 7*C*, available at www.jneurosci.org as supplemental material), we estimate a K_D of 2.72 ($\pm$0.19) $\times 10^{-6}$ mol/L for GCAP2–RIBEYE interaction.

To test whether RIBEYE also interacts with GCAP2 *in situ*, we performed coimmunoprecipitation experiments using extracts from the bovine retina. In these experiments, GCAP2 immune serum but not GCAP2 preimmune serum coimmunoprecipitated RIBEYE (Fig. 4*A*), again demonstrating the specificity of the interaction. Identical results were obtained when RIBEYE antibodies were used for immunoprecipitation. RIBEYE immune serum but not RIBEYE preimmune serum specifically coimmunoprecipitated GCAP2 (Fig. 4*B*). The coimmunoprecipitation experiments suggest that the RIBEYE–GCAP2 interaction also occurs *in situ* in the retina and emphasize the physiological relevance of the RIBEYE–GCAP2 interaction. This assumption is further supported by our findings that GCAP2 is also a component of purified synaptic ribbons as shown both with a polyclonal as well as with the monoclonal GCAP2 antibody (Fig. 4*B*, lane 4; supplemental Fig. 3*A*,*B*,*F*, available at www.jneurosci.org as supplemental material).

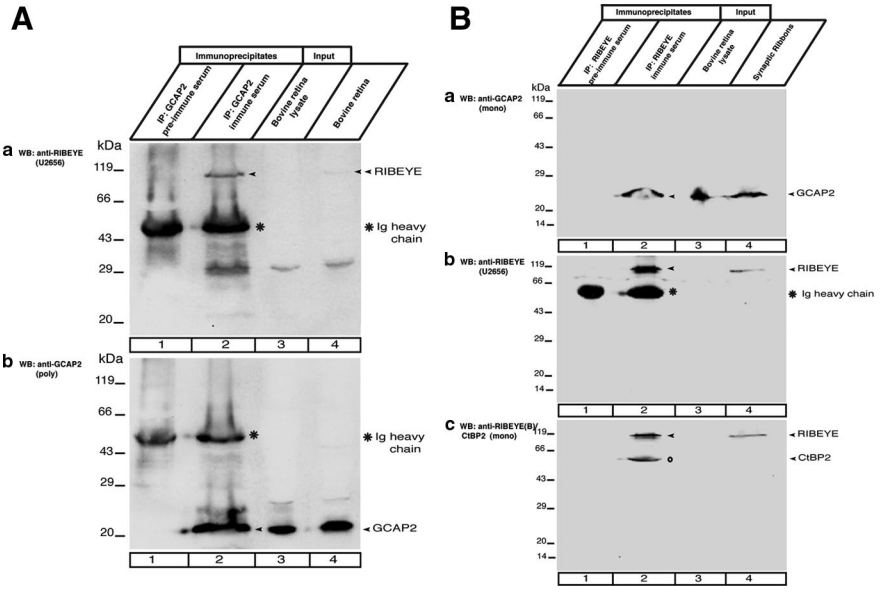

Figure 4. Coimmunoprecipitation of RIBEYE and GCAP2 from the bovine retina. ***Aa***, GCAP2 immune serum and GCAP2 preimmune serum were tested for their capability to coimmunoprecipitate RIBEYE. The experiments were analyzed by SDS-PAGE (12.5% polyacrylamide gels) followed by Western blotting (WB) with the indicated antibodies. RIBEYE is coimmunoprecipitated by GCAP2 immune serum (lane 2, arrowhead) but not by GCAP2 preimmune serum (lane 1). ***Ab***, The same blot as in ***Aa*** but reprobed with rabbit polyclonal anti-GCAP2 antibodies. This blot shows the presence of GCAP2 precipitated by the immune serum (lane 2, arrowhead) but not by the preimmune serum (lane 1). Asterisks indicate the immunoglobulin heavy chains. ***B***, RIBEYE immune serum and RIBEYE preimmune serum were tested for their capability to coimmunoprecipitate GCAP2. The experiments were analyzed by SDS-PAGE (12.5% polyacrylamide gels) followed by Western blotting with the indicated antibodies. GCAP2 is coimmunoprecipitated by RIBEYE immune serum (***Ba***, lane 2, arrowhead) but not by RIBEYE preimmune serum (***Ba***, lane 1). ***Bb***, The same blot as in ***Ba*** but reprobed with polyclonal anti-RIBEYE (U2656). RIBEYE was immunoprecipitated by the RIBEYE immune serum (lane 2, arrowhead) but not by the RIBEYE preimmune serum (lane 1). Asterisks indicate the immunoglobulin heavy chains. ***Bc***, The same blot as in ***Bb*** but reprobed with mouse monoclonal anti-CtBP2 antibodies which detect the B domain of RIBEYE. Similar to ***Bb***, this blot also shows the presence of RIBEYE precipitated by the RIBEYE immune serum (lane 2) but not by the RIBEYE preimmune serum (lane 1). In addition to RIBEYE, an additional protein at ~50 kDa is present in the experimental precipitate (lane 2) but not in the control immunoprecipitate (lane 1). This 50 kDa band very likely is CtBP2 (***Bc***, lane 2, circle). Purified synaptic ribbons contain RIBEYE and CtBP1 but not CtBP2 (K.S. and F.S., unpublished data). In the input lanes (lane 3), 0.5% of total input was loaded in ***A***, and 1% of total input in ***B***. The immunoprecipitates are always 100%. In the input lanes ("bovine retina lysate"; ***A***, ***B***, lane 3), RIBEYE is only visible as a faint band because RIBEYE is not a major protein in the crude retinal lysate prepared as described in Materials and Methods, and only a limited amount of protein can be loaded on a single lane. The "bovine retina lysate" contains the Triton X-soluble supernatant after tissue extraction and spinning at 13,000 rpm (30 min, 4°C; see Materials and Methods). RIBEYE is strongly enriched in the experimental immunoprecipitates (***Aa***, ***Bb***, ***Bc***, lane 2). Lane 4 in ***Ab*** serves as positive control. In ***A***, lane 4 is loaded with (total) bovine retina boiled in sample buffer; in ***B***, lane 4 is loaded with purified synaptic ribbons. IP, Immunoprecipitation.

RIBEYE and GCAP2 colocalize in photoreceptor ribbon synapses of the mammalian retina

Next, we performed immunolabeling experiments with a polyclonal GCAP2 antibody raised against bacterially expressed and purified full-length bovine GCAP2 as well as with a commercial monoclonal mouse GCAP2 antibody (Figs. 5*A–F*, 6; Table 1; supplemental Figs. 3*A–C*,*F*, 4*B*, 5, 6, available at www.jneurosci.org as supplemental material). Similar to the findings from other groups (Otto-Bruc et al., 1997, Cuenca et al., 1998; Kachi et al., 1999), we observed a strong GCAP2 immunolabeling in the synaptic terminals of bovine photoreceptors in addition to a strong expression particularly in the inner segments (Fig. 5*A–F*; supplemental Fig. 8*F*, available at www.jneurosci.org as supplemental material). A strong immunolabeling of the rod presynaptic terminals was observed (Fig. 5; supplemental Fig. 5, available at www.jneurosci.org as supplemental material); the labeling of the larger cone terminals was less intense (supplemental Fig. 5, available at www.jneurosci.org as supplemental material). Double immunolabeling demonstrated that RIBEYE and GCAP2 colocalized in the presynaptic terminals of photoreceptors (Figs. 5*B–E*, 6). GCAP2 was found at synaptic ribbon sites (immunolabeled by RIBEYE antibodies) and close to synaptic ribbons (Figs. 5, 6). Most but not all ribbons were labeled (Fig. 5; supplemental Figs. 5, 6, available at www.jneurosci.org as supplemental material). The GCAP2 immunosignals were specific because the signal could be completely blocked by preabsorbing the polyclonal antiserum with GCAP2-GST fusion protein but not GST protein alone (supplemental Figs. 3*C*, 6, available at www.jneurosci.org as supplemental material). Furthermore, identical results, as described above for the polyclonal GCAP2 antibody, were obtained with a commercially available monoclonal antibody against GCAP2 (Fig. 5*D*,*E*) that does not cross-react with GCAP1 (supplemental Fig. 3*F*, available at www.jneurosci.org as supplemental material). The polyclonal GCAP2 antibody raised against full-length GCAP2 cross-reacts with GCAP1 (supplemental Fig. 4*B*, available at www.jneurosci.org as supplemental material). Therefore, we analyzed whether GCAP1 interacts with RIBEYE in the YTH system. We found that RIBEYE(B) interacts only with the CTR of GCAP2 but not with the CTR of GCAP1 (supplemental Fig. 4*C*, available at www.jneurosci.org as supplemental material), indicating that RIBEYE specifically interacts with GCAP2 but not with GCAP1 (supplemental Fig. 4*C*, available at www.jneurosci.org as supplemental material). Qualitatively identical results as de-

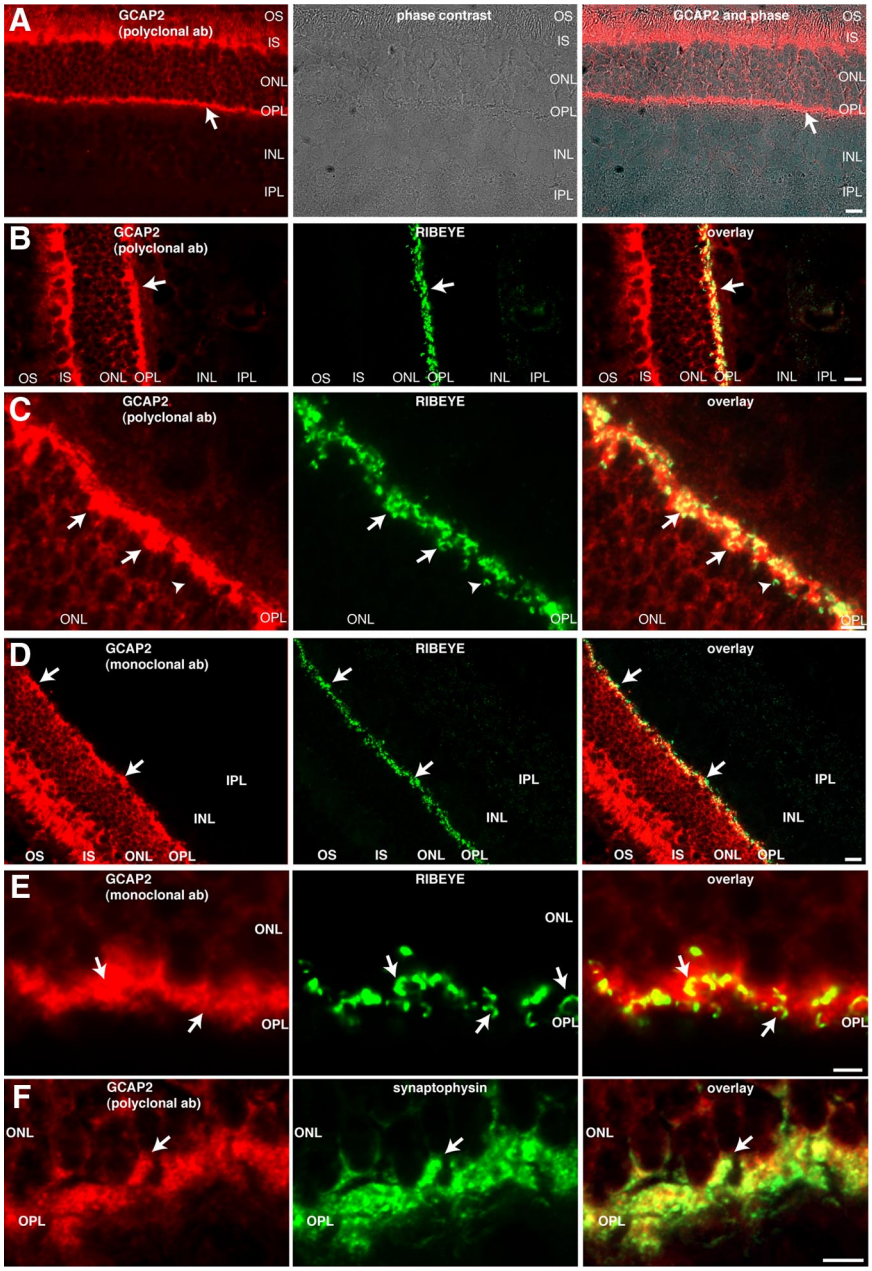

Figure 5. GCAP2 colocalizes with synaptic ribbons in photoreceptor ribbon synapses (as analyzed by conventional epifluorescence microscopy). ***A–E***, Immunolabeling of the bovine retina with rabbit polyclonal antibodies against GCAP2 (***A–C***) and mouse monoclonal antibodies against RIBEYE(B)/CtBP2 (***B***, ***C***), or mouse monoclonal antibodies against GCAP2 (clone A1; Santa Cruz Biotechnology) and rabbit polyclonal antibodies against RIBEYE (U2656) (***D***, ***E***). Both the polyclonal (***A–C***) as well as the monoclonal (***D***) GCAP2 antibodies generated a strong immunolabel particularly in the inner segments (ISs) of bovine photoreceptor cells. In addition, the OPL that contains photoreceptor ribbon synapses is strongly labeled by the polyclonal (***A–C***) and monoclonal GCAP2 antibodies (***D***, ***E***). The OPL, which is immunolabeled by the GCAP2 antibodies, is labeled by arrows in ***A*** and ***B***. The GCAP2 immunosignal colocalized with synaptic ribbons, which were visualized by immunolabeling with RIBEYE antibodies (***B–E***, arrows). Strong immunosignals of GCAP2 were found at synaptic ribbons and in close vicinity to synaptic ribbons. Most, but not all, ribbons colocalized with GCAP2. The arrowhead in ***C*** denotes synaptic ribbons that were not associated with detectable amounts of GCAP2. ***F***, The GCAP2 immunosignal in the OPL mostly colocalizes with the immunosignal of synaptophysin, a marker protein of synaptic vesicles highly enriched in the presynaptic terminals (arrow). Virtually identical results as described above for the bovine retina were also obtained for the mouse retina (Fig. 6; supplemental Fig. 8, available at www.jneurosci.org as supplemental material). OS, Outer segment; IPL, inner plexiform layer. Scale bars: ***A***, ***B***, ***D***, 15 μm; ***C***, ***E***, ***F***, 10 μm.

scribed above for immunolabeling of the bovine retina with polyclonal and monoclonal antibodies against GCAP2 were also obtained for the mouse retina (Fig. 6*A*,*B*; supplemental Fig. 8*A–E*, available at www.jneurosci.org as supplemental material). In the distal parts of the photoreceptors, the GCAP2 immunosignals were typically stronger in the inner segments compared to the outer segments. This was the case in the light-adapted bovine and mouse retina (Fig. 5*A*,*B*,*D*; supplemental Fig. 8*A*,*B*,*F*, available at www.jneurosci.org as supplemental material). High-resolution confocal laser scanning microscopy showed a clear colocalization between RIBEYE and GCAP2 signals, demonstrating that GCAP2 and synaptic ribbons are in close proximity to each other (Fig. 6).

RIBEYE and GCAP2 are localized very close to each other in photoreceptor synapses as judged by *in situ* PLA

The close association of RIBEYE and GCAP2 *in situ* was further supported by *in situ* PLAs (Gustafsdottir et al., 2005) on flash-frozen mouse retinal sections (Fig. 7). PLA *in situ* interaction assays critically depend on the close proximity of the interaction partners (Söderberg et al., 2006). In PLAs, the secondary antibodies are labeled with specific oligonucleotides. Only if the two antigens detected by two different primary antibodies are in close proximity to each other (<40 nm) can a linker oligonucleotide hybridize to the distinct PLUS/MINUS oligonucleotides conjugated to the secondary antibodies and provide the template for a rolling circle amplification (Söderberg et al., 2006, 2008). The product of the rolling circle amplification is then specifically detected by a fluorescent oligonucleotide probe (Fig. 7). In the case of RIBEYE and GCAP2, a strong PLA interaction signal was observed in the outer plexiform layer (OPL) (Fig. 7*A–E*). There was no interaction signal present in the OPL if both primary antibodies were omitted or if only one primary antibody was applied (followed by incubation with the two oligonucleotide-conjugated secondary antibodies), demonstrating the specificity of the detection assay. As an additional negative control, RIBEYE and opsin were tested for interaction by PLA and did not produce any signal in the OPL, further demonstrating specificity of the PLA interaction assays (Fig. 7*J*). In contrast, a mixture of rabbit polyclonal RIBEYE (U2656) and mouse monoclonal CtBP2 antibodies (positive control) gave a strong PLA interaction system in the OPL (Fig. 7*L*). Remarkably, RIBEYE and mGluR6 did not produce a PLA interaction signal in the OPL (Fig. 7*M*). RIBEYE at the synaptic ribbon and mGluR6 at the tips of invaginating ON bipolar cells of the ribbon synapse obviously are not close enough to produce a PLA interaction signal, further emphasizing the very close proximity of GCAP2 and synaptic ribbons in the presynaptic terminal *in situ* (see Discussion).

In conclusion, using different independent assays, we have shown that RIBEYE interacts with GCAP2 in the synaptic terminals of photoreceptor cells.

Characterization of RIBEYE(B)–GCAP2 binding

To further characterize binding of GCAP2 to RIBEYE, we analyzed why the presence of 1 mM βME is essential for RIBEYE–GCAP2 interaction in the fusion protein pull-down experiments (Fig. 3). If βME was absent from the incubation buffer, RIBEYE(B) did not bind to GCAP2-GST in the fusion protein pull-down assays (Figs. 8*A*,*B*, 9*A*–*D*; supplemental Fig. 7*A*,*B*, available at www.jneurosci.org as supplemental material). It is well known that βME can cleave disulfide bridges (for review, see Berg et al., 2007). Rat RIBEYE(B) domain contains eight cysteine residues: RIBEYE (B)C587; RIBEYE(B)C603; RIBEYE(B)C667; RIBEYE(B)C683; RIBEYE(B)C781; RIBEYE (B)C786; RIBEYE(B)C861, and RIBEYE(B) C899. From these cysteines, only cysteine C667 and cysteine C899 in the SBD of RIBEYE are predicted to be close enough to form disulfide bridges in monomeric RIBEYE (Fig. 8*D*,*E*). RIBEYE(B)C667 is located in SBDa spatially close to RIBEYE(B)C899 in the SBDb, and a disulfide bridge between these residues would thus link the two different parts of the SBD with each other. We analyzed RIBEYE(B)C899S for its capability to interact with GCAP2 and tested whether this RIBEYE point mutant needs βME to interact with GCAP2 in pull-down assays. Most interestingly, RIBEYE(B)C899S interacted with GCAP2 in the absence of βME (Fig. 8*B*), demonstrating that RIBEYE(B)C899S does not need βME to bind to GCAP2. Similarly, RIBEYE(B)C667S, the putative partner of RIBEYE(B)C899S for disulfide bridge formation, also interacted with RIBEYE(B) in the absence of β-mercaptoethanol in protein pull-down analyses (supplemental Fig. 7*A*, available at www.jneurosci.org as supplemental material). We suggest that these cysteine residues, RIBEYE(B)C667 and RIBEYE(B)C899, which are located very close (within a few amgstroms) to each other (Fig. 8*D*,*E*), form a disulfide bridge that restricts movement of the SBD relative to the NBD, and thus also the conformational freedom of the connecting hinge 2 region (see Discussion). Mutating RIBEYE(B)C683 (which is located in the homodimerization interface of the NBD) (Fig. 8*D*) into RIBEYE(B)C683S did not change the dependency of GCAP2/RIBEYE interaction from the presence of βME (Fig. 8*A*, lanes 7,8), demonstrating that only specific cysteine mutations of RIBEYE(B) lead to an independence from βME for GCAP2 binding.

RIBEYE(B)C899S and RIBEYE(B)C667S, which were shown to be important in modulating GCAP2–RIBEYE interaction (Fig. 8*B*,*D*,*E*; supplemental Fig. 7*A*, available at www.jneurosci.org as supplemental material), are located in the SBD of RIBEYE(B). We also tested noncysteine mutants of the SBD—namely, RIBEYE(B)F904W and RIBEYE(B)ΔCTR—for their capability to interact with GCAP2. RIBEYE(B)F904 is located in the SBDb at the end of the modeled structure (Figs. 1*B*, 2*A*,*B*, 8*D*,*E*). RIBEYE(B)ΔCTR lacks the hydrophobic C-terminal region (CTR; aa912-918 of RIBEYE); the structure of the CTR has not yet been resolved (Kumar et al., 2002; Nardini et al., 2003). RIBEYE(B)F904W and RIBEYE(B)ΔCTR did not interact with GCAP2 in the YTH system, although these mutants are not within the proper binding region of RIBEYE for GCAP2 (Figs. 2, 8*C*–*E*). We interpret these data to mean that the latter mutants of the SBD are likely not relevant for a direct physical interaction with GCAP2 but are less well capable to stabilize a conformation of the hinge 2 region that can bind GCAP2 (see Discussion).

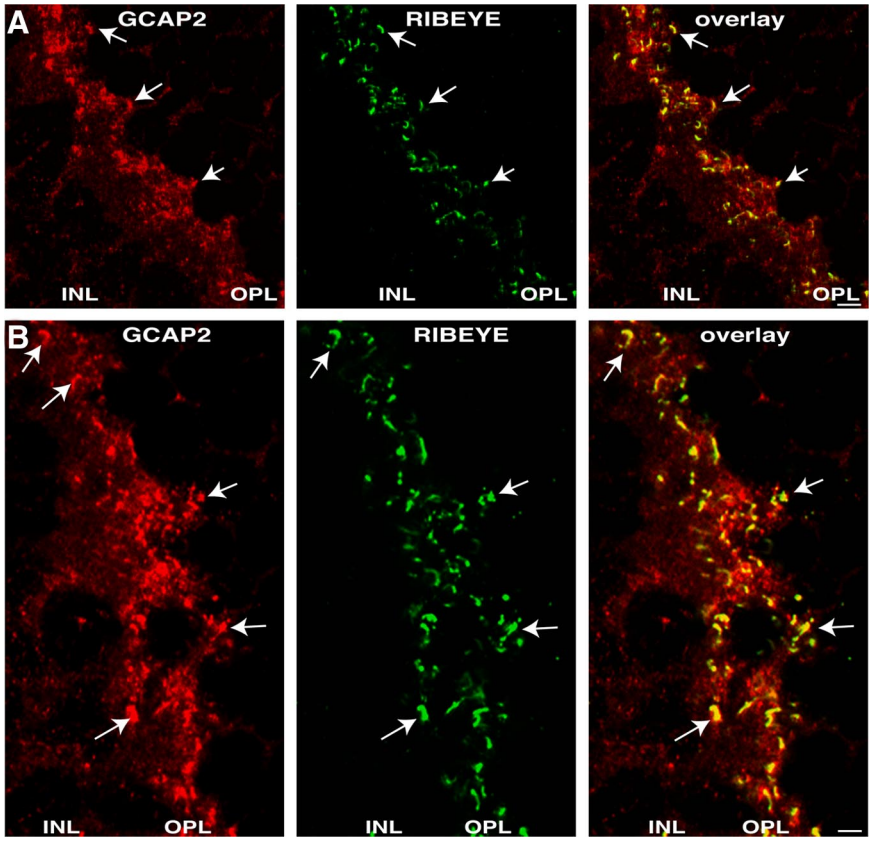

Figure 6. GCAP2 colocalizes with synaptic ribbons in photoreceptor ribbon synapses (as analyzed by confocal laser scanning fluorescence microscopy). ***A***, ***B***, Immunolabeling of the mouse retina with rabbit polyclonal antibodies against GCAP2 and mouse monoclonal antibodies against RIBEYE(B)/CtBP2 as analyzed by confocal laser scanning microscopy. GCAP2 colocalizes with synaptic ribbons that are immunolabeled with antibodies against RIBEYE. Arrows point to examples of RIBEYE-labeled synaptic ribbons that are also immunoreactive for GCAP2. INL, inner nuclear layer. Scale bars: 5 μm.

RIBEYE(B)–GCAP2 interaction is NADH dependent

We tested whether the reducing power of βME is important in promoting RIBEYE–GCAP2 interaction. RIBEYE(B) efficiently binds reduced NADH (Schmitz et al., 2000; Alpadi et al., 2008). Therefore, we analyzed whether NADH could replace βME in promoting RIBEYE–GCAP2 interaction. Indeed, GCAP2 bound to RIBEYE(B) in the absence of βME if NADH was present in the incubation buffer (Fig. 9*A*,*C*; supplemental Fig. 7*Bb*, available at www.jneurosci.org as supplemental material). Surprisingly, also the oxidized form of NADH, NAD^+, induced RIBEYE(B)–GCAP2 interaction in the absence of βME (Fig. 9*B*,*D*; supplemental Fig. 7*Ba*), demonstrating that the reducing power of NADH does not play a major role in promoting GCAP2–RIBEYE interaction. Both the oxidized as well as the reduced form of NADH (NAD^+ and NADH, respectively) stimulate RIBEYE–GCAP2 interaction. The NADH concentrations applied in these experiments are perfectly within the known physiological range

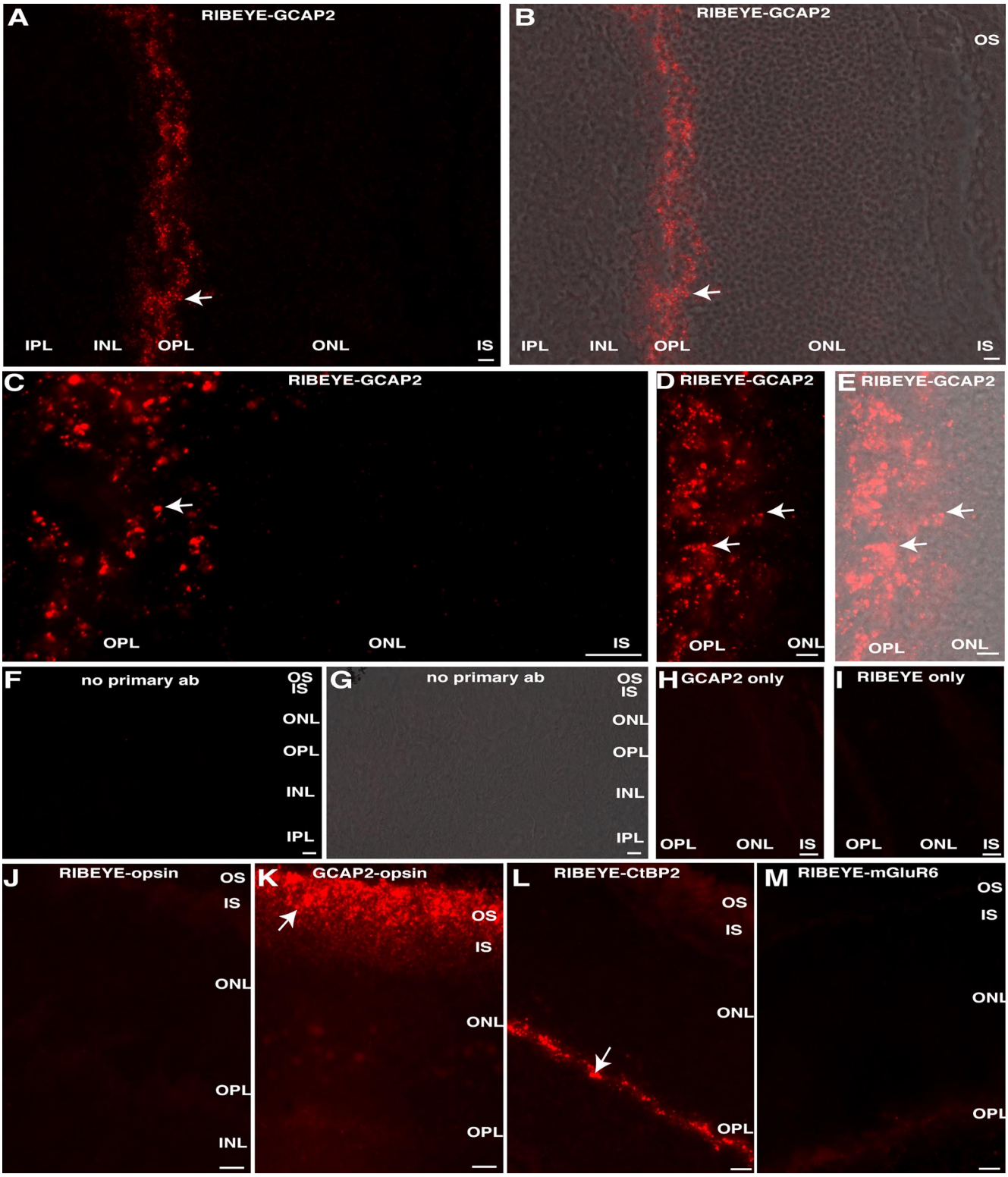

Figure 7. Colocalization of RIBEYE and GCAP2 as analyzed by *in situ* PLAs. Colocalization of RIBEYE and GCAP2 in retinal sections *in situ* was analyzed using proximity ligation assays (Gustafsdottir et al., 2005; Söderberg et al., 2008). This assay critically depends on the distance of the interaction partners and a positive PLA interaction signal is only generated if the interaction partners are located in a distance of $<$40 nm (Söderberg et al., 2006). ***A–E***, A strong PLA interaction signal in the OPL, as visualized by the red fluorescence signal, was observed between RIBEYE and GCAP2. ***A***, ***B***, An overview of the PLA signals is given at a low magnification. ***C–E***, High-magnifications of the OPL. In ***B*** and ***E***, the PLA signals of ***A*** and ***D*** are superimposed onto the respective phase images. Arrows point to PLA interaction signals in the OPL indicating close proximity of RIBEYE and GCAP2. ***F–I***, No PLA interaction signal was present in the OPL if both primary antibodies were omitted (***F***, ***G***) or if only one primary antibody was applied (***H***, ***I***), demonstrating the specificity of the detection assay. ***G***, The PLA signal of ***F*** is superimposed onto the respective phase image. ***J***, As an additional negative control, RIBEYE and opsin were tested for interaction by PLA and did not produce any signal in the OPL, again demonstrating specificity of the PLA interaction assays. ***K***, ***L***, In contrast, a mixture of RIBEYE (U2656)/CtBP2 antibodies (positive control) gave a strong PLA interaction signal in the OPL (***L***). A mixture of GCAP2/opsin antibodies generated a strong PLA interaction signal in the outer/inner segments (ISs) but not in the OPL (***K***). ***M***, RIBEYE and mGluR6, which are located relatively closely together but beyond the critical distance of PLAs of $\sim$40 nm (Söderberg et al., 2006), did not produce a PLA interaction signal in the OPL, demonstrating that PLA interaction signals clearly indicate very close proximity of the analyzed antigens. Arrows in ***K*** and ***L*** point to PLA interaction signals. INL, inner nuclear layer; IPL, inner plexiform layer. Scale bars: ***A–M***, 10 μm.

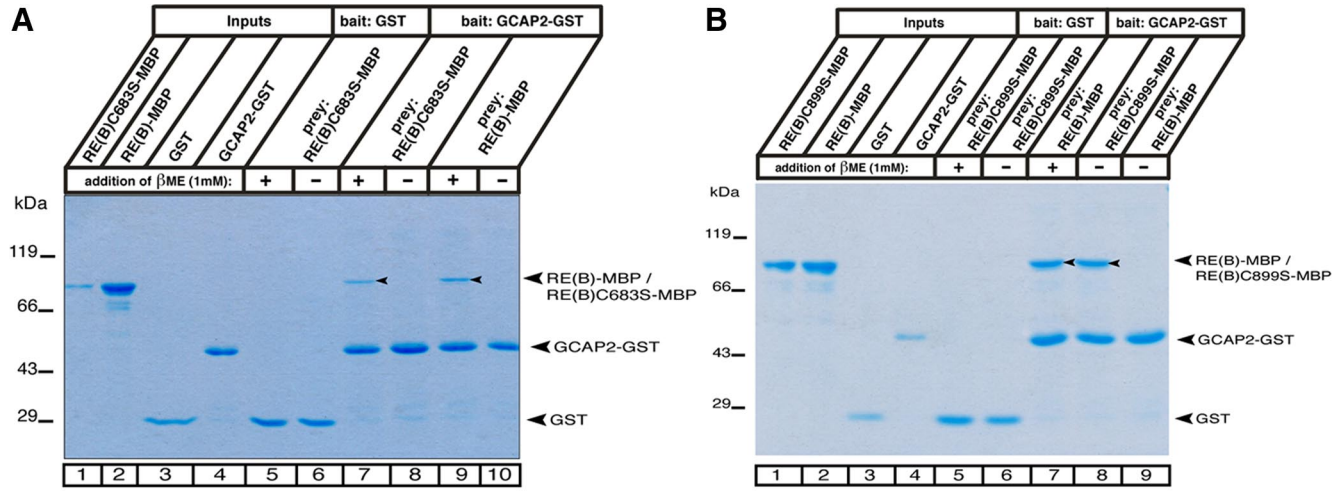

C Mutations in the SBD of RIBEYE influence the binding of GCAP2 to RIBEYE(B)

	mating	bait	prey	-ALWH	βGal
1		RE(B)F904W	GCAP2(3-204)	–	–
2		RE(B)F904W	pACT2	–	–
3		RE(B)F904W	pSE1111	–	–
4		pGBKT7	GCAP2(3-204)	–	–
5		pSE1112	GCAP2(3-204)	–	–
6		RE(B)	GCAP2(3-204)	+	+
7		RE(B)ΔCTR	GCAP2(3-204)	–	–
8		RE(B)ΔCTR	pACT2	–	–
9		RE(B)ΔCTR	pSE1111	–	–
10		RE(B)F904W	RE(B)	+	+

D Localization of cysteine residues in RIBEYE(B)

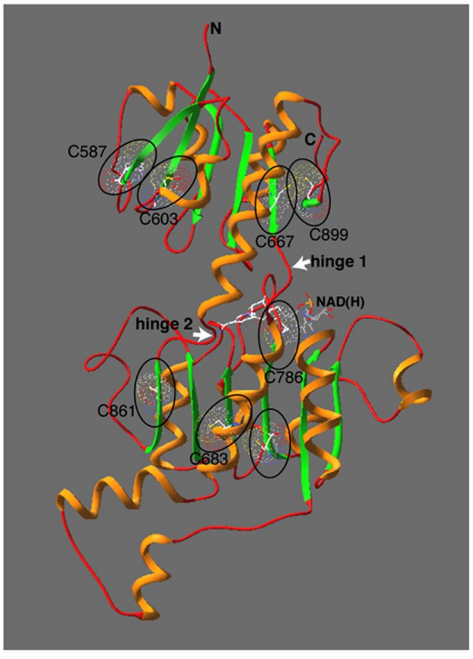

E A disulfide bridge between C667 and C889 restricts movement of the SBDb and hinge 2 relative to SBDa

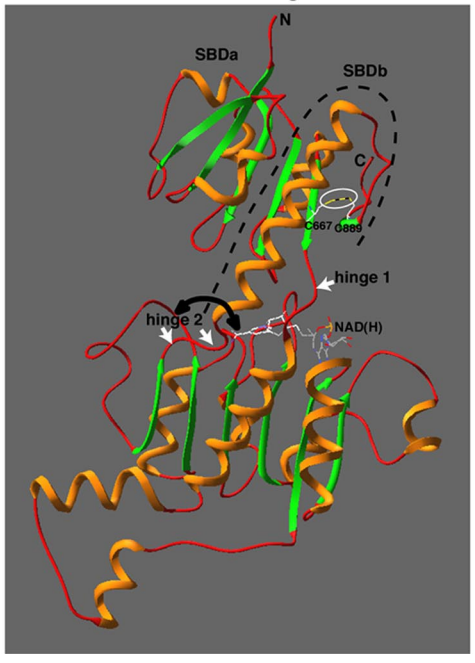

Figure 8. The binding of GCAP2 to the hinge 2 region of RIBEYE(B) [RE(B)] is modulated by the SBD of RIBEYE(B). ***A***, ***B***, Fusion protein pull-down assays analyzed by SDS-PAGE (10% acrylamide gels). ***A***, GCAP2 does not pull down both wild-type RE(B) or RE(B)C683S in the absence of βME (lanes 8, 10) but only if βME is present (lanes 7, 9; arrowheads). ***B***, In contrast, GCAP2 pulls down RIBEYE(B)C899S in the absence of βME (lane 8, arrowhead). ***C***, Point-mutating F904 in RIBEYE(B) to RE(B)F904W abolishes RIBEYE(B)–GCAP2 interaction in the YTH system (mating 1). Similarly, deleting the hydrophobic CTR of RIBEYE(B) results in a lack of interaction between RIBEYE and GCAP2 in the YTH system (mating 7). ***D***, Localization of cysteine residues in RIBEYE(B). Only cysteine C667 and cysteine C899 are located within a distance of ~4 Å to form a disulfide bridge (indicated by overlapping black circles). ***E***, A predicted disulfide bridge between C667 in SBDa and C889 in SBDb (white circle) can be expected to limit the rotational freedom of the hinge 2 region and the movement of the SBDb relative to SBDa (black, curved arrow). The structure model in ***D*** and ***E*** starts at amino acid P575 and ends at amino acid F905 of RIBEYE, and is based on the crystal structure of tCtBP1 (Kumar et al., 2002; Nardini et al., 2003; see also Alpadi et al., 2008; Magupalli et al., 2008). ALWH, Dropout medium lacking adenine, leucine, tryptophan, and histidine; LW, dropout medium lacking leucine and tryptophan.

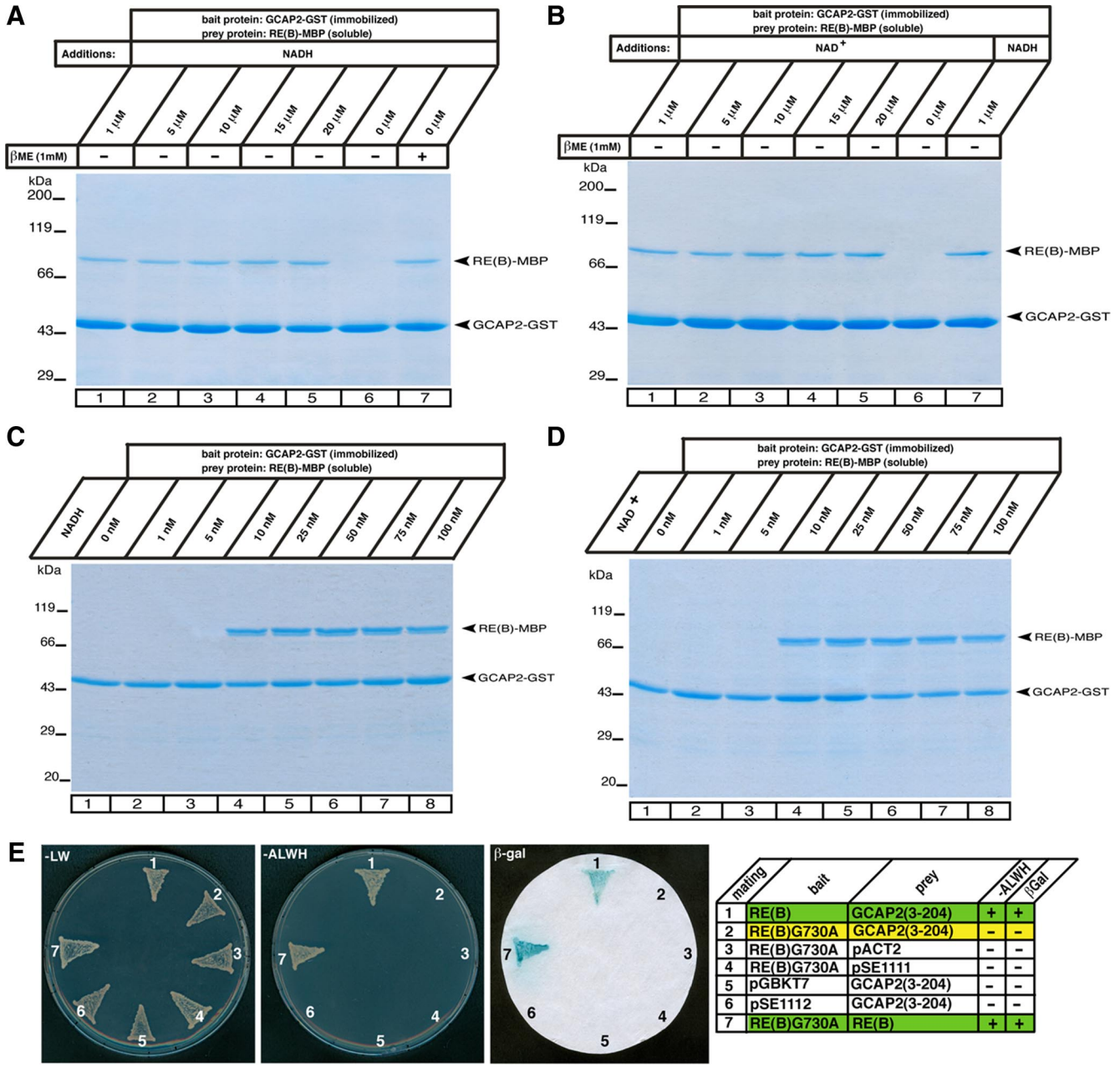

mating	bait	prey	-ALWH	βGal
1	RE(B)	GCAP2(3-204)	+	+
2	RE(B)G730A	GCAP2(3-204)	–	–
3	RE(B)G730A	pACT2	–	–
4	RE(B)G730A	pSE1111	–	–
5	pGBKT7	GCAP2(3-204)	–	–
6	pSE1112	GCAP2(3-204)	–	–
7	RE(B)G730A	RE(B)	+	+

Figure 9. NADH and NAD $^+$ are essential cofactors for the binding between RIBEYE and GCAP2 in the absence of βME. In the fusion protein pull-down analyses the fusion proteins were used at an equimolar concentration of 0.8 μM. Fusion protein pull-down assays were analyzed by SDS-PAGE (10% acrylamide gels). RIBEYE(B) [RE(B)] binds NADH with high affinity (Schmitz et al., 2000). ***A***, ***B***, In fusion protein pull-down assays, GCAP2–RIBEYE(B) interaction requires the presence of βME. If βME is absent, GCAP2 does not bind to RIBEYE(B) unless NADH or NAD $^+$ is added to the incubation buffer. Both the reduced form (NADH) (***A***) as well as the oxidized form (NAD $^+$; ***B***) promote RIBEYE(B)–GCAP2 interaction. ***C***, ***D***, Low concentrations of NADH promote RIBEYE/GCAP2 interaction. We tested whether low concentrations of NADH (***C***) or NAD $^+$ (***D***) [ranging from 0.001 μM (1 nM) to 0.1 μM (100 nM)] were able to stimulate binding of RIBEYE to GCAP2 in the absence of βME. NAD $^+$/NADH promoted RIBEYE(B)–GCAP2 binding already at concentrations as low as 10 nM (***C***, ***D***, lane 4). If still lower concentrations of NADH were used, i.e., 1 and 5 nM (***C***, ***D***, lanes 2, 3, respectively), interaction was no longer observed, similar to the absence of interaction in the absence of any NADH (***C***, lane 1) or NAD $^+$ (***D***, lane 1). The incubation buffer in the experiments shown above (***A–D***) did not contain any βME. ***E***, To further evaluate the importance of NADH in promoting RIBEYE(B)–GCAP2 interaction, we analyzed the NADH-binding-deficient RIBEYE point mutant, RIBEYE(B)G730A (Alpadi et al., 2008; Magupalli et al., 2008) in the YTH system for interaction with GCAP2. In agreement with the essential requirement of NADH in promoting RIBEYE/GCAP2 interaction in fusion protein pull-down analyses, GCAP2 did not bind to the NADH-binding-deficient RIBEYE point mutant RIBEYE(B)G730A in the YTH system as judged by the lack of growth on −ALWH selective medium and lack of β-galactosidase (β-gal) expression (mating 2). Mating 1 indicates a positive control [RIBEYE(B) mated with GCAP2]. Matings 3–6 show the respective autoactivation controls. RIBEYE(B)G730A is still able to homodimerize with wild-type RIBEYE(B), demonstrating that RIBEYE(B)G730A is not misfolded (mating 7). For convenience, experimental bait–prey pairs are underlayered in color (green, interacting bait–prey pairs; yellow, noninteracting bait–prey pairs); control matings are not colored. ALWH, Dropout medium lacking adenine, leucine, tryptophan, and histidine; LW, dropout medium lacking leucine and tryptophan.

of intracellular NADH concentrations (Zhang et al., 2002; Fjeld et al., 2003). The necessity of NADH binding to RIBEYE for GCAP2–RIBEYE interaction was further demonstrated by the analysis of a NADH binding-deficient RIBEYE mutant: RIBEYE (B)G730A (Magupalli et al., 2008). GCAP2 did not interact with this NADH binding-deficient RIBEYE point mutant in the YTH system (Fig. 9*E*), although this RIBEYE point mutant was able to efficiently heterodimerize with RIBEYE(B) wild-type protein (Fig. 9*E*).

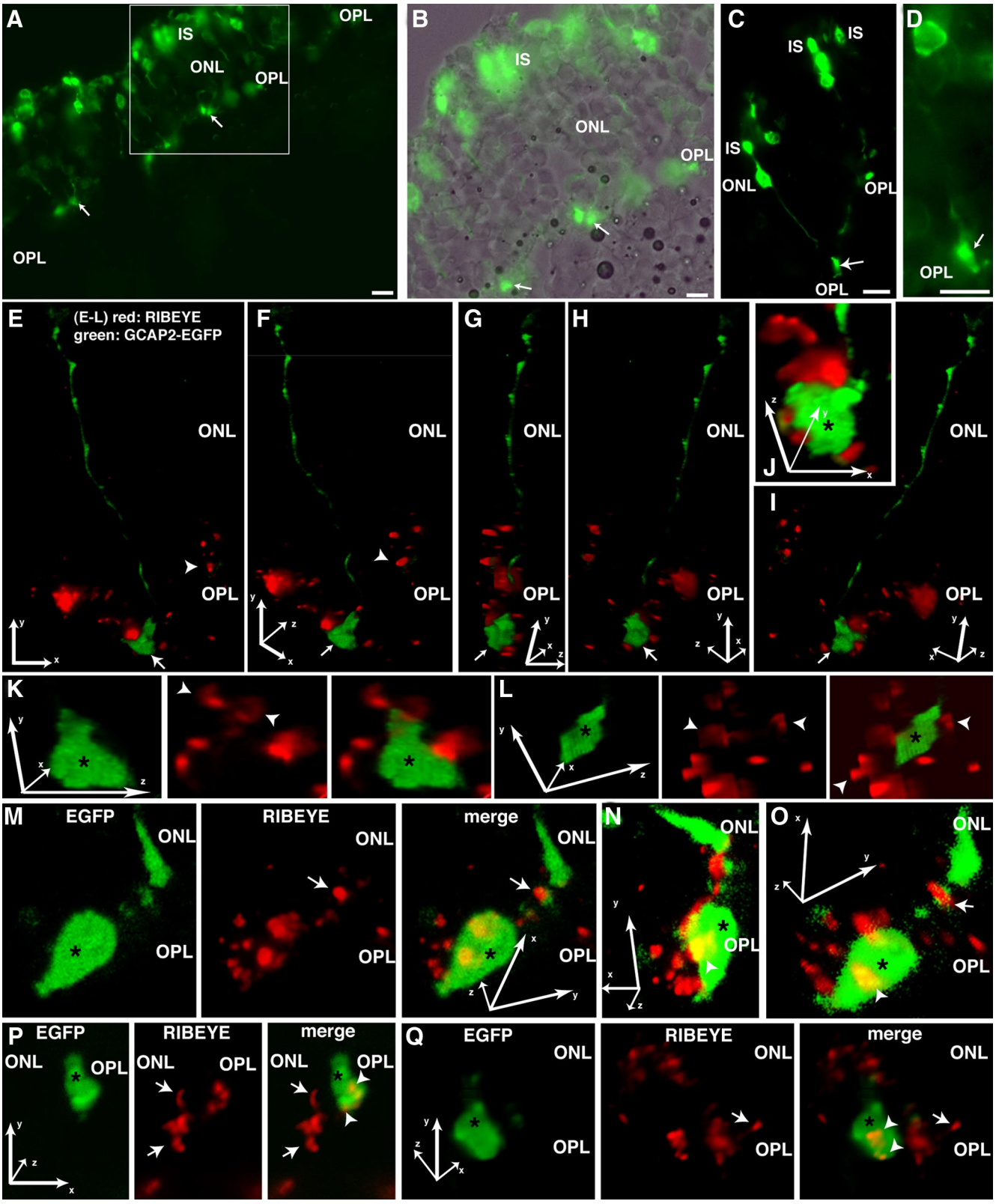

Figure 10. Overexpression of GCAP2 in photoreceptor terminals disassembles synaptic ribbons. ***A–D***, Recombinant expression of either GCAP2-EGFP or EGFP in organotypic retina explant cultures. SLF virus efficiently infects photoreceptors in organotypical explant cultures of the retina. SLF-mediated GCAP2-EGFP (***A–C***) heterologous expression labels the entire photoreceptor from the inner segments to the synaptic terminals (arrows) in the OPL. As generally observed by us and other groups (Fischer et al., 2000; Perez-Leon et al., 2003; Zhang et al., 2008), outer segments are absent from explant preparations. In analogy to GCAP2-EGFP expression, infection with EGFP-SLF virus also leads to labeling of the entire photoreceptor (***D***) in retina explant culture. Scale bars: ***A–D***, 10 μm. ***E–Q***, Three-dimensional reconstructions of individual optical stacks along the *z*-axis of SLF-virus-infected retina explant recorded with the Apotome (Zeiss). To visualize synaptic ribbons in GCAP2-EGFP- and EGFP-infected retina explants, samples were immunolabeled with polyclonal RIBEYE antibody (U2656; red signals). Synaptic ribbons are abundantly present in the OPL of the organotypical retina cultures (***E–L***, arrowheads) but absent from GCAP2-EGFP-expressing photoreceptor terminals (***E–I***, white arrows; ***J–Q***, asterisks). ***E–I*** show lower magnifications of a three-dimensional reconstructed GCAP2-EGFP expressing photoreceptor from different angles to emphasize the lack of synaptic ribbons within the terminal (white arrows) without influencing the presence of synaptic ribbons (*Figure legend continues*.)

Viral overexpression of GCAP2 in presynaptic photoreceptor terminals promotes disassembly of photoreceptor synaptic ribbons

It is well established that the dynamics of synaptic ribbons is dependent on intracellular Ca^{2+} (Spiwoks-Becker et al., 2004). Synaptic ribbons tend to disassemble via spherical disassembly intermediates in response to illumination in the mouse retina when intracellular Ca^{2+} is low. Noteworthy, the disassembly of synaptic ribbons could be experimentally induced by chelating extracellular Ca^{2+} with EGTA/BAPTA (Spiwoks-Becker et al., 2004). Therefore, we tested whether GCAP2 could possibly be involved in these well-known Ca^{2+}-dependent dynamic changes of synaptic ribbons and analyzed whether synaptic GCAP2 expression could be related to the Ca^{2+}-dependent dynamic changes of synaptic ribbons.

For this purpose, we generated recombinant GCAP2-EGFP expressing SLF virus and used this recombinant virus for infecting retinal explants. EGFP-expressing SLF virus served as control virus. In organotypic retinal explant cultures, the recombinant SLF viruses preferentially infected photoreceptors (Fig. 10*A–D*). Photoreceptors were infected at a high density with the SLF viruses (Fig. 10*A*, *B*) and showed expression of GCAP2-EGFP (Fig. 10*C*) or EGFP (Fig. 10*D*) throughout all photoreceptor cell compartments including the synaptic terminals (Fig. 10). Our organotypical cultures did no longer contain outer segments as also observed in other organotypic retinal cultures. Interestingly, photoreceptor terminals that were infected with GCAP2-EGFP virus typically displayed a loss of synaptic ribbons as analyzed by coimmunolabeling with RIBEYE antibodies (U2656) (Fig. 10*E–L*). Photoreceptor terminals infected with EGFP virus (control virus) did not show loss of synaptic ribbons, indicating that the loss of synaptic ribbons in GCAP2-EGFP-infected photoreceptors is not attributable to a cytopathic effect of the virus infection itself (Fig. 10*M–Q*). In EGFP-infected photoreceptors, 77.3 ± 3.8% SD (482 synapses counted from four independent retinal cultures) of the synaptic terminals contained synaptic ribbons, whereas in GCAP2-EGFP-infected photoreceptors, only 30.1 ± 4.5% SD (389 synapses from four independent cultures) contained synaptic ribbons in their synaptic terminals as judged by RIBEYE immunolabeling. The same observation described above for the light microscopic analyses was also observed at the electron microscopic level using electron microscopic analyses of GCAP2-EGFP and EGFP (control)-infected retinas (Fig. 11). In GCAP2-EGFP-infected retinas, we observed a dramatic reduction in the number of synaptic ribbons in photoreceptor terminals in comparison to photoreceptor terminals of EGFP-infected control retinas [EGFP-infected retinas, 1.092 bar-shaped synaptic ribbons (longer than >150 nm) per photoreceptor synaptic terminal (±0.091 SD; $n = 181$ synapses from six independent cultures); GCAP2-EGFP-infected retinas, 0.164 bar-shaped synaptic ribbons (longer than >150 nm) per photoreceptor synaptic terminal (±0.033 SD, $n = 181$ synapses from six independent cultures].

Discussion

GCAP2 is a photoreceptor-enriched neuronal Ca^{2+}-sensor protein. Its role as a Ca^{2+}-dependent modulator of the phototransduction cascade is well known (for review, see Palczewski et al., 2004). Previous studies have shown that GCAP2 is not restricted to photoreceptor outer and inner segments, but is also present in photoreceptor presynaptic terminals (Otto-Bruc et al., 1997; Duda et al., 2002, Pennesi et al., 2003; Makino et al., 2008). The function of GCAP2 in photoreceptor synapses is not known. The analyses of GCAP2 knock-out mice suggested a synaptic function of GCAPs based on electroretinogram analyses that showed a defect in the b-wave of the electroretinogram (Pennesi et al., 2003). But the mechanism by which GCAPs might work in the synapse remained unclear. In the present study, we show with many different, independent approaches that GCAP2 binds to RIBEYE, the major component of synaptic ribbons in the active zone of photoreceptor synapses, and is involved in synaptic ribbon dynamics. The selective association of GCAP2 with photoreceptor synaptic ribbons but not with bipolar cell synaptic ribbons further contributes to known physiological differences between different types of retinal ribbon synapses (e.g., Heidelberger et al., 1994; von Gersdorff and Matthews, 1994; Neves and Lagnado, 1999; Thoreson et al. 2004; Innocenti and Heidelberger, 2008; Sheng et al., 2007; Schmitz, 2009).

RIBEYE–GCAP2 interaction requires structural rearrangements of RIBEYE(B) domain

Our YTH mapping analyses demonstrated that the hinge 2 region of RIBEYE(B) is responsible for the interaction with the CTR of GCAP2. This suggestion is further supported by point mutants of the hinge 2 region that abolished interaction with GCAP2. The hinge 2 region is structurally flexible, and its conformation is regulated by NADH binding and also by dimerization. This has been shown for various members of the D-isomer-specific hydroxyacid dehydrogenase family to which also RIBEYE belongs (Goldberg et al., 1994; Lamzin et al., 1994; Kumar et al., 2002; Nardini et al., 2003; for review, see Popov and Lamzin, 1994; Chinnadurai, 2002). NADH-binding induces movement of the SBD toward to the NBD via rotation around the hinge regions resulting in closure of the NADH binding cleft ("closed" conformation). Additionally, binding of NADH results in the structural organization of the CTR. The NADH-induced creation of a new α-helix that interacts with NADH stabilizes the "closed" conformation.

Thus, we suggest that binding of GCAP2 to the hinge 2 region of RIBEYE(B) requires the NADH-induced, closed conformation of RIBEYE(B). This hypothesis can explain the NADH-induced stimulation of GCAP2 binding and provides an explanation for the observed modulatory role of the SBD: the NADH-induced closed conformation requires considerable structural rearrangements in the SBD and movement of both SBDa and SBDb. The predicted disulfide bridge between C667 and C899 locks SBDb to SBDa and restricts the movements of the two portions of the SBD relative to each other (Fig. 8*E*). Therefore, the observed capability of RIBEYE(B)C899S and RIBEYE(B)C667S to bind GCAP2 in the absence of βME could be attributed to an enhanced conformational flexibility of the SBD. In these mutants, a disulfide

←

(*Figure legend continued.*) (***E***, ***F***, ***K***, ***L***, arrowheads) in the neighboring noninfected photoreceptors. The x, y, and z labeled arrows indicate the coordinate axes in the three dimensions and are scaled to represent the distance of 5 μm in each spacial direction. ***J–L***, High magnifications of GCAP2-EGFP infected photoreceptor terminals. Although many synaptic ribbons (red signals; ***E***, ***F***, ***K***, arrowheads) can be detected next to the GCAP2 virus-infected terminals (asterisks), no synaptic ribbons are present within the GCAP2-overexpressing terminals. The synaptic terminals are labeled by white arrows in ***E*** and ***F***, and by asterisks in ***K*** and ***L***. ***M–Q***, Lack of synaptic ribbons within GCAP2-infected photoreceptor terminals is not caused by a cytopathic effect of virus infection as such, because terminals overexpressing EGFP alone do contain synaptic ribbons as visualized by the yellow color within the EGFP-expressing synaptic terminals (***N–Q***, arrowheads). Arrows in ***M–Q*** are synaptic ribbons that are located outside of virus-infected terminals. ***N***, ***O***, Views of the same infected, EGFP-expressing terminal as in ***M***, but from different angles. IS, Inner segments; ONL, outer nuclear layer.

bridge can no longer be formed between RIBEYE(B)C899 and RIBEYE(B)C667. This enhanced flexibility of the SBD will facilitate movement of the SBD toward the NBD. We propose that this enhanced flexibility of the SBD favors formation of the closed conformation of the hinge 2 region that can subsequently bind GCAP2.

The incapability of the RIBEYE(B) mutants RIBEYE(B)F904W and RIBEYE (B)ΔCTR to bind to GCAP2 can be explained by a decreased capability of these mutants to stabilize the closed conformation. RIBEYE(B)ΔCTR lacks the hydrophobic CTR of RIBEYE(B), which undergoes enormous structural rearrangements after NADH binding (Lamzin et al., 1994; Nardini et al., 2003). RIBEYE(B)F904 is located at the beginning of the CTR in the SBD of RIBEYE(B) (Magupalli et al., 2008). The CTR has an important role in stabilizing the closed conformation in the D-isomer-specific 2-hydroxyacid dehydrogenase protein family (Lamzin et al., 1994). We propose that the decreased GCAP2 binding of these CTR mutants is based on their decreased capability to stabilize the closed conformation.

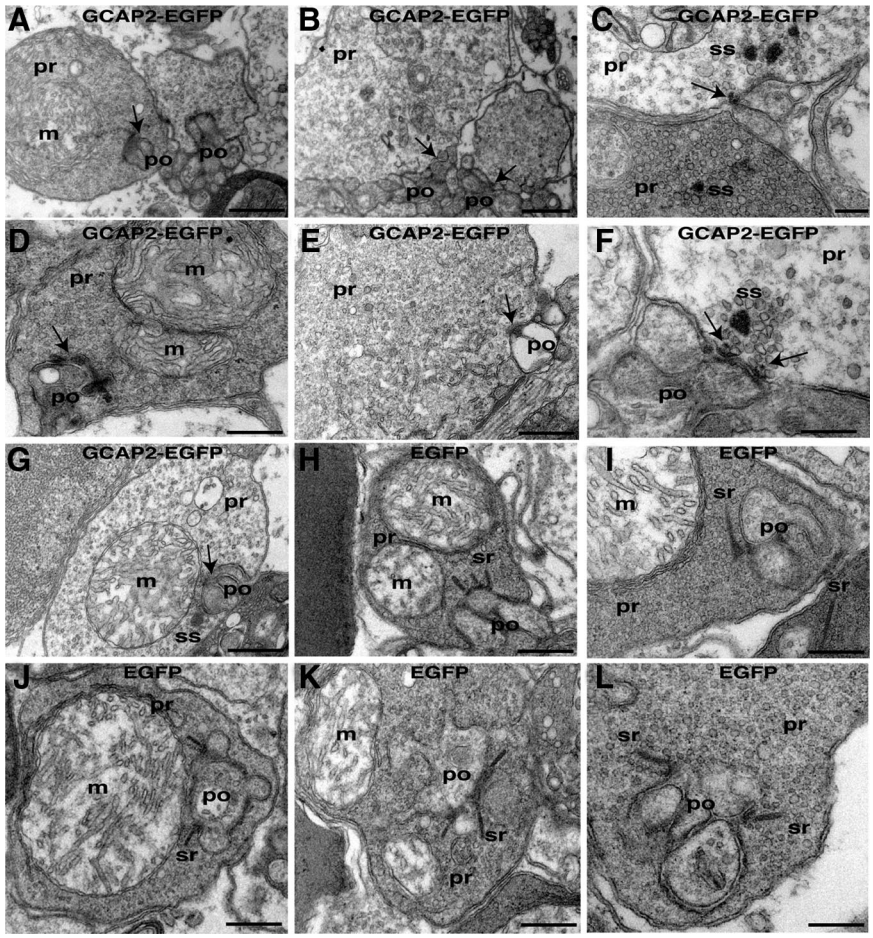

Figure 11. Overexpression of GCAP2 in photoreceptor terminals disassembles synaptic ribbons. Electron microscopic analyses are shown. ***A–L***, Expression of either GCAP2-EGFP (***A–G***) or EGFP in organotypic retina explant cultures by the respective recombinant viruses (***H–L***) (see also Fig. 10). Seven representative images of photoreceptor synapses from GCAP2-EGFP-infected retinas are shown in ***A–G***; five representative images of photoreceptor synapses from EGFP-infected retinas are shown in ***H–L*** (control infections). Infection with GCAP-EGFP (***A–G***) leads to a loss of synaptic ribbons at the presynaptic active zones (arrows). In many cases, instead of bar-shaped anchored synaptic ribbons, floating, nonanchored spherical synaptic ribbons (ss) were observed, which are considered as intermediate stages in the disassembly of synaptic ribbons. EGFP-infected photoreceptors (control infections; ***H–L***) displayed normal photoreceptor terminals with normal-looking bar-shaped synaptic ribbons. pr, Presynaptic terminal; po, postsynaptic dendrites; sr, synaptic ribbon; m, mitochondrion. Scale bars: ***A***, ***B***, ***D***, ***E***, 1 μm; ***C***, 250 nm; ***F***, ***G–L***, 500 nm.

The regulation of RIBEYE/GCAP2 interaction *in situ*

We have shown that NADH and NAD^+ are similarly effective in promoting RIBEYE/GCAP2 interaction. Very low concentrations of NADH (down to 10 nM) induced the binding of GCAP2 to RIBEYE. Since both the oxidized and reduced form of NADH are equally effective, the binding of GCAP2 to RIBEYE and synaptic ribbons does probably not critically depend on the metabolic state/redox state of the presynaptic terminal. Several proteins (e.g., E1A, ZEB) are known that interact with CtBP proteins in a redox-sensitive manner (Zhang et al., 2002; Garriga-Canut et al., 2006). The different redox sensitivities of these interactions are probably based on different binding sites. Whereas GCAP2 binds to the hinge 2 region of RIBEYE(B) in a redox-insensitive manner (this study), redox-sensitive interaction partners (e.g., E1A and ZEB) bind to a hydrophobic portion in the SBD in some distance from the hinge 2 region (Zhang et al., 2002; Nardini et al., 2003; Kuppuswamy et al., 2008). Binding of NADH is usually accompanied by dimerization of CtBP proteins (Balasubramanian et al., 2003; Thio et al., 2004; Nardini et al., 2009). Currently, we cannot discriminate whether binding of NADH to RIBEYE is the only or main event that promotes RIBEYE/GCAP2 interaction in the synapse or whether the dimerization of RIBEYE(B) is also involved. Both events (NADH binding and dimerization) are interconnected with each other and are expected to promote the closed conformation of RIBEYE(B). Additional factors, i.e., certain kinases such as p21-activated kinase 1 (Pak1) that were suggested to regulate dimerization and NADH-binding (Barnes et al., 2003) could also be relevant for the induction of GCAP2 binding. Since NADH binding and dimerization are tightly linked, we speculate that both events could promote interaction of RIBEYE with GCAP2 *in situ*. The concentrations of NADH in the presynaptic photoreceptor terminal and at the synaptic ribbon itself are unknown. Also, possible fluctuations in NADH concentrations in response to light and dark stimulations that could be particularly relevant for structural changes of synaptic ribbons during light and dark adaption have not yet been investigated so far. But regardless from these limitations, the concentrations necessary to promote RIBEYE/GCAP2 interaction are low and within the known physiological range of cellular NADH concentrations (Fjeld et al., 2003).

GCAP2, a candidate to mediate Ca^{2+}- and illumination-dependent synaptic ribbon dynamics

The number and shape of synaptic ribbons are dynamic in nature, and structural changes of synaptic ribbons are important determinants of synaptic performance (Hull et al., 2006; Johnson et al., 2008; Meyer et al., 2009). Spiwoks-Becker et al. (2004) demonstrated disassembly of synaptic ribbons in photoreceptor terminals during illumination when exocytosis is low. Illumina-

tion of photoreceptors also reduces the presynaptic Ca^{2+} concentration in photoreceptor ribbon terminals (Jackman et al., 2009). Interestingly, the tendency of synaptic ribbons to disassemble during environmental illumination could be mimicked by removing (chelating) extracellular Ca^{2+}, indicating that Ca^{2+} is an important mediator of synaptic ribbon dynamics. We propose that GCAP2 mediates the known Ca^{2+}-dependent structural changes of synaptic ribbons during light and darkness.

As mentioned above, Ca^{2+} is needed to maintain the structural integrity of synaptic ribbons, and consequently, chelating of Ca^{2+}, e.g., by GCAP2 that has been recruited to RIBEYE via a NADH-dependent mechanism at the synaptic ribbon, could reduce number and/or size of synaptic ribbons. Viral overexpression of GCAP2 in photoreceptors reduced the number of synaptic ribbons (present study), qualitatively similar to chelating extracellular Ca^{2+} (Spiwoks-Becker et al., 2004). The stronger ribbon disassembly in GCAP2-overexpressing photoreceptors is not surprising because intracellular overexpression of a Ca^{2+}-binding protein can be expected to induce a stronger effect than the indirect manipulation of intracellular Ca^{2+} through chelation of extracellular Ca^{2+}.

In addition to a mechanism that is based on Ca^{2+}-buffering, GCAP2 could also exert its function by alternative molecular mechanisms: GCAP2 binds to guanylate cyclases in the outer segments in a Ca^{2+}-dependent manner during phototransduction and light-/dark adaptation. Based on several findings (Liu et al., 1994, Rieke and Schwartz, 1994; Cooper et al., 1995; Savchenko et al., 1997, Duda et al., 2002; Müller et al., 2003; Venkataraman et al., 2003; Spiwoks-Becker et al., 2004; Zhang et al., 2005), GCAP2 could possibly also influence guanylate cyclases in the presynaptic photoreceptor terminals. Based on that thinking, GCAP2 could regulate the activity of synaptic guanylate cyclases, which in turn could regulate synaptic ribbon structure, e.g., via cGMP-dependent mechanisms. Photoreceptor terminals express guanylate cyclases (Liu et al., 1994, Cooper et al., 1995; Duda et al., 2002; Venkataraman et al., 2003), and studies on synaptic ribbons of the pineal gland strongly support a role for cGMP in synaptic ribbon dynamics (for review, see Vollrath and Spiwoks-Becker, 1996). By this way of thinking, the modulation of synaptic cGMP levels and guanylate cyclases by GCAP2 would appear to be an alternative molecular mechanism that could regulate synaptic ribbon dynamics. The further characterization of GCAP2-dependent synaptic functions and mechanisms, i.e., whether pure Ca^{2+} buffering or modulation of enzymatic activity or both regulate ribbon structure, and the modulation of GCAP2-effector interactions by intracellular Ca^{2+} and NADH in the synapse, remain to be elucidated by future analyses.

References

Alpadi K, Magupalli VG, Käppel S, Köblitz L, Seigel GM, Sung CH, Schmitz F (2008) RIBEYE recruits Munc119, a mammalian ortholog of the *Caenorhabditis elegans* protein unc119, to synaptic ribbons of photoreceptor synapses. J Biol Chem 283:2641–26467.

Ames JB, Dizhoor AM, Ikura M, Palczewski K, Stryer L (1999) Three-dimensional structure of guanylyl cyclase activating protein-2, a calcium-sensitive modulator of photoreceptor guanylyl cyclases. J Biol Chem 274:19329–19337.

Ashery U, Betz A, Xu T, Brose N, Rettig J (1999) An efficient method for the infection of adrenal chromaffin cells using the Semliki Forest virus gene expression system. Eur J Cell Biol 78:525–532.

Balasubramanian P, Zhao LJ, Chinnadurai G (2003) Nicotinamide adenine dinucleotide stimulates oligomerization, interaction with E1A and an intrinsic dehydrogenase activity of CtBP. FEBS Lett 537:157–160.

Barnes CJ, Vadlamudi RK, Mishra SK, Jacobson RH, Liu F, Kumar R (2003) Functional inactivation of a transcriptional corepressor by a signalling kinase. Nat Struct Biol 10:622–628.

Berg JM, Tymoczko JL, Stryer L (2007) Biochemistry, Ed 6. New York: Freeman.

Chinnadurai G (2002) CtBP, an unconventional transcriptional corepressor in development and oncogenesis. Mol Cell 9:213–224.

Cooper N, Liu L, Yoshida A, Pozdnyakiv N, Margulis A, Sitaramaya A (1995) The bovine rod outer segment guanylate cyclase, ROS-GC, is present in both outer segments and synaptic layers of the retina. J Mol Neurosci 6:211–222.

Cuenca N, Lopez S, Howes K, Kolb H (1998) The localization of guanylyl cyclase-activating proteins in the mammalian retina. Invest Ophthalmol Vis Sci 39:1243–1250.

Duda T, Koch KW, Venkataraman V, Lange C, Beyermann M, Sharma RK (2002) Ca^{2+} sensor S100beta-modulated sites of membrane guanylate cyclase in the photoreceptor–bipolar synapse. EMBO J 21:2547–2556.

Fischer F, Kneussel M, Tintrup H, Haverkamp S, Rauen T, Betz H, Wässle H (2000) Reduced synaptic clustering of GABA and glycine receptors in the retina of the gephyrin null mutant mouse. J Comp Neurol 42:634–648.

Fjeld CC, Birdsong WT, Goodman RH (2003) Differential binding of NAD+ and NADH allows the transcriptional corepressor carboxyl-terminal binding protein to serve as a metabolic sensor. Proc Natl Acad Sci U S A 100:9202–9207.

Garriga-Canut M, Schoenike B, Qazi R, Bergendahl K, Daley TJ, Pfender RM, Morrison JF, Ockuly J, Starfstrom C, Sutula T, Roopra A (2006) 2-Deoxy-D-glucose reduces epilepsy progression by NRSF-CtBP-dependent metabolic repression of chromatin structure. Nat Neurosci 9:1382–1387.

Goldberg JD, Yoshida T, Brick P (1994) Crystal structure of a NAD-dependent D-glycerate dehydrogenase at 2.4A resolution. J Mol Biol 236:1123–1140.

Gustafsdottir SM, Schallmeiner E, Fredriksson S, Gullberg M, Söderberg O, Jarvius M, Jarvisu J, Howell M, Landegren U (2005) Proximity ligation assays for sensitive and specific protein analyses. Anal. Biochem 345:2–9.

Heidelberger R, Heinemann C, Neher E, Matthews G (1994) Calcium dependence of the rate of exocytosis in a synaptic terminal. Nature 371:513–515.

Heidelberger R, Thoreson WB, Witkovsky P (2005) Synaptic transmission at retinal ribbon synapses. Prog Retin Eye Res 24:682–720.

Hull C, Studholme K, Yazulla S, von Gersdorff H (2006) Diurnal changes in exocytosis and the number of synaptic ribbons at active zones of an ON-type bipolar cell terminal. J Neurophysiol 96:2025–2033.

Imanishi Y, Li N, Sokal I, Sowa ME, Lichtarge O, Wensel TG, Saperstein DA, Baehr W, Palczewski K (2002) Characterization of retinal guanylate cyclase-activating protein 3 (GCAP3) from zebrafish to man. Eur J Neurosci 15:63–78.

Innocenti B, Heidelberger R (2008) Mechanisms contributing to tonic release at the cone photoreceptor ribbon synapse. J Neurophysiol 99:25–36.

Jackman SL, Choi SY, Thoreson WB, Rabl K, Bartoletti TM, Kramer RH (2009) Role of the synaptic ribbon in transmitting the cone light response. Nat Neurosci 12:303–310.

Johnson SL, Forge A, Knipper M, Münkner S, Marcotti W (2008) Tonotopic variation in the calcium dependence of neurotransmitter release and vesicle pool replenishment at mammalian auditory ribbon synapses. J Neurosci 28:7670–7678.

Kachi S, Nishizawa Y, Olshevskaya E, Yamazaki A, Miyake Y, Wakabayashi T, Dizhoor AM, Usukura J (1999) Detailed localization of photoreceptor guanylate cyclase activating protein-1 and -2 in mammalian retinas using light and electron microscopy. Exp Eye Res 68:465–473.

Koch KW, Duda T, Sharma RK (2002) Photoreceptor specific guanylate cyclases in vertebrate phototransduction. Mol Cell Biochem 230:97–106.

Kumar V, Carlson JE, Ohgi KA, Edwards TA, Rose DW, Escalante CR, Rosenfeld MG, Aggarwal AK (2002) Transcription corepressor CtBP is an NAD^+-regulated dehydrogenase. Mol Cell 10:857–869.

Kuppuswamy M, Vjayalingam S, Zhao L-J, Zhou Y, Subramanian T, Ryerse J, Chinnadurai G (2008) Role of the PLDLS-binding cleft region of CtBP1 in recruitment of core and auxiliary components of the corepressor complex. Mol Cell Biol 28:269–281.

Lamzin VS, Dauter Z, Popov VO, Harutyunyan EH, Wilson KS (1994) High resolution structures of holo and apo formate dehydrogenase. J Mol Biol 236:759–785.

Liu X, Seno K, Nishizawa Y, Hayashi F, Yamazaki A, Matsumoto H, Wakabayashi T, Usukura J (1994) Ultrastructural localization of retinal guanylate cyclase in human and monkey retinas. Exp Eye Res 59:761–768.

Magupalli VG, Schwarz K, Alpadi K, Natarajan S, Seigel GM, Schmitz F (2008) Multiple RIBEYE–RIBEYE interactions create a dynamic scaffold for the formation of the synaptic ribbons. J Neurosci 28:7954–7967.

Makino CL, Peshenko IV, Wen XH, Olshevskaya EV, Barrett R, Dizhoor AM (2008) A role for GCAP2 in regulating the photoresponse: guanylyl cyclase activation and rod electrophysiology in GUCA1B knockout mice. J Biol Chem 283:29135–29143.

Meyer AC, Frank T, Khimich D, Hoch G, Riedel D, Chapochnikow NM, Yarin YM, Harke B, Hell SW, Egner A, Moser T (2009) Tuning of synapse number, structure and function in the cochlea. Nat Neurosci 4:444–453.

Müller F, Schotten A, Ivanova E, Haverkamp S, Kremmer E, Kaupp UB (2003) HCN channels are expressed differentially in retinal bipolar cells and concentrated at synaptic terminals. Eur J Neurosci 17:2084–2096.

Nardini M, Spano S, Cericola C, Pesce A, Massaro A, Millo E, Luini A, Corda D, Bolognesi M (2003) CtBP/BARS: a dual function protein involved in transcription co-repression and Golgi membrane fission. EMBO J 22:3122–3130.

Nardini M, Valente C, Ricagno S, Luini A, Corda D, Bolognesi M (2009) CtBP1/BARS Gly172-Glu mutant structure: impairing NAD(H)-binding. Biochem Biophys Res Commun 381:70–74.

Neves G, Lagnado L (1999) The kinetics of exocytosis and endocytosis in the synaptic terminal of goldfish retinal bipolar cells. J Physiol 515:181–202.

Olshevskaya EV, Hughes RE, Hurley JB, Dizhoor AM (1997) Calcium binding, but not a calcium-myristoyl switch, controls the ability of guanylyl cyclase-activating protein GCAP2 to regulate photoreceptor guanylyl cyclase. J Biol Chem 272:14327–14333.

Otto-Bruc A, Fariss RN, Haeseleer F, Huang J, Buczylko J, Surgocheva I, Baehr W, Milam AH, Palczewski K (1997) Localization of guanylate cyclase-activating protein 2 in mammalian retina. Proc Natl Acad Sci U S A 94:4727–4732.

Palczewski K, Sokal I, Baehr W (2004) Guanylate cyclase-activating proteins: structure, function and diversity. Biochem Biophys Res Commun 7:161–164.

Pennesi ME, Howes KA, Baehr W, Wu SM (2003) Guanylate cyclase-activating protein (GCAP) 1 rescues cone recovery kinetics in GCAP1/GCAP2 knockout mice. Proc Natl Acad Sci U S A 100:6783–6788.

Pérez-León J, Frech MJ, Schröder JE, Fischer F, Kneussel M, Wässle H, Backus KH (2003) Spontaneous synaptic activity in an organotypi culture of the mouse retina. Invest Ophthalmol Vis Sci 44:1376–1387.

Popov VO, Lamzin VS (1994) NAD^+-dependent formate dehydrogenase. Biochem J 301:625–643.

Rieke F, Schwartz EA (1994) A cGMP-gated current can control exocytosis in cone synapses. Neuron 13:863–879.

Savchenko A, Barnes S, Kramer RH (1997) Cyclic-nucleotide-gated channels mediate synaptic feedback by nitric oxide. Nature 390:694–698.

Schmitz F (2009) The making of synaptic ribbons: how they are built and what they do. Neuroscientist 15:611–624.

Schmitz F, Bechmann M, Drenckhahn D (1996) Purification of synaptic ribbons, structural components of the photoreceptor active zone complex. J Neurosci 16:7109–7116.

Schmitz F, Königstorfer A, Südhof TC (2000) RIBEYE, a component of synaptic ribbons. A proteins journey through evolution provides insight into synaptic ribbon function. Neuron 28:857–872.

Schmitz F, Tabares L, Khimich D, Strenzke N, de la Villa-Polo P, Castellano-Munoz M, Bulankina A, Moser T, Fernandez-Chacon R, Südhof TC (2006) CSPα deficiency causes massive and rapid photoreceptor degeneration. Proc Natl Acad Sci U S A 103:2926–2931.

Schoch S, Mittelstaedt T, Kaeser P, Padgett D, Feldmann N, Chevaleyre V, Castillo PE, Hammer RE, Han W, Schmitz F, Lin W, Südhof TC (2006) Redundant functions of RIM1alpha and RIM2 alpha in Ca^{2+}-triggered neurotransmitter release. EMBO J 25:5852–5863.

Sheng Z, Choi S, Dharia A, Li L, Sterling P, Kramer RH (2007) Synaptic Ca^{2+} is lower in rods than cones, causing slower tonic release of vesicles. J Neurosci 27:5033–5042.

Söderberg O, Gullberg M, Jarvisu M, Ridderstrale K, Leuchowius KJ, Jarvius I, Wester K, Hydbrig P, Bahram F, Larsson LG, Landegren U (2006) Direct observation of individual endogenous protein complexes in situ by proximity ligation. Nat Methods 3:995–1000.

Söderberg O, Leuchowius K-J, Gullberg M, Jarvius M, Weibrecht I, Larsson LG, Landegren (2008) Characterizing proteins and their interactions in cells and tissues using the *in situ* proximity ligation assay. Methods 45:227–232.

Spiwoks-Becker I, Glas M, Lasarzik I, Vollrath L (2004) Mouse photoreceptor synaptic ribbons lose and regain material in response to illumination changes. Eur J Neurosci 19:1559–1571.

Sterling P, Matthews G (2005) Structure and function of ribbon synapses. Trends Neurosci 28:20–29.

Thio SS, Bonventre JV, Hsu SI (2004) The CtBP2 co-repressor is regulated by NADH-dependent dimerization and possesses a novel N-terminal repression domain. Nucleic Acids Res 32:1836–1847.

Thoreson WB, Rabl K, Townes-Anderson E, Heidelberger R (2004) A highly Ca^{2+}-sensitive pool of vesicles contributes to linearity at the the rod photoreceptor ribbon synapse. Neuron 42:595–605.

tom Dieck S, Brandstätter JH (2006) Ribbon synapses of the retina. Cell Tissue Res 326:339–346.

Venkataraman V, Duda T, Vardi N, Koch K-W, Sharma RK (2003) Calcium-modulated guanylate cyclase transduction machinery in the photoreceptor bipolar synaptic region. Biochemistry 42:5640–5648.

Vollrath L, Spiwoks-Becker L (1996) Plasticity of retinal ribbon synapses. Microsc Res Tech 35:472–487.

von Gersdorff H, Matthews G (1994) Inhibition of endocytosis by elevated internal calcium in a synaptic terminal. Nature 370:652–655.

Wan L, Almers W, Chen W (2005) Two ribeye genes in teleosts: the role of ribeye in ribbon formation and bipolar cell development. J Neurosci 25:941–949.

Zenisek D, Horst NK, Merrifield C, Sterling P, Matthews G (2004) Visualizing synaptic ribbons in the living Cell. J Neurosci 24:9752–9759.

Zhang M, Marshall B, Atherton SS (2008) Murine cytomegalovirus infection and apoptosis in organotypic retinal cultures. Invest Ophthalmol Vis Sci 49:295–303.

Zhang N, Beuve A, Townes-Anderson E (2005) The nitric oxide–cGMP signaling pathway differentially regulates presynaptic structural plasticity in cone and rod cells. J Neurosci 25:2761–2770.

Zhang Q, Piston DW, Goodman RH (2002) Regulation of corepressor function by nuclear NADH. Science 295:1895–1897.